Physics 129 LECTURE 11 February 11, 2014

- Early Universe Cosmology
  - Three Pillars of the Big Bang: Expansion, CMB, Big Bang Nucleosynthesis
  - Cosmic Radiation: Relativistic Massive Particles, Photons, and Neutrinos
  - Decoupling of Neutrinos, After e^+e^- Annihilation $T_\nu = (4/11)^{1/3}\ T_\gamma$
  - Big Bang Nucleosynthesis
  - Abundance of Atomic Matter - Five Different Methods Agree
  - Abundance of ^{4}He
  - Abundance of Deuterium - New, High-precision Measurement
  - Abundance of 7Li, Possibly Indicating New Physics
  - Formation of the Elements; Stellar Archeology

The in-class open-book Midterm Exam will be Thursday February 13.

I will be away Wed-Fri, so my Wed office hour is cancelled this week.

Successful Predictions of the Big Bang

First Prediction	First Confirmation
Expansion of the Universe	
Friedmann 1922, Lemaitre 1927 based on Einstein 1916	Hubble 1929
Cosmic Background Radiation	
Existence of CBR Gamow, Alpher, Hermann 1948	Penzias & Wilson 1965
CBR Thermal Spectrum Peebles 1966	COBE 1989
CBR Fluctuation Amplitude Cold Dark Matter theory 1984	COBE 1992
CBR Acoustic Peak	BOOMERANG 2000 MAXIMA 2000
Light Element Abundances	
Peebles 1966, Wagoner 1967	D/H Tytler et al. 1997

Three Pillars of the Big Bang

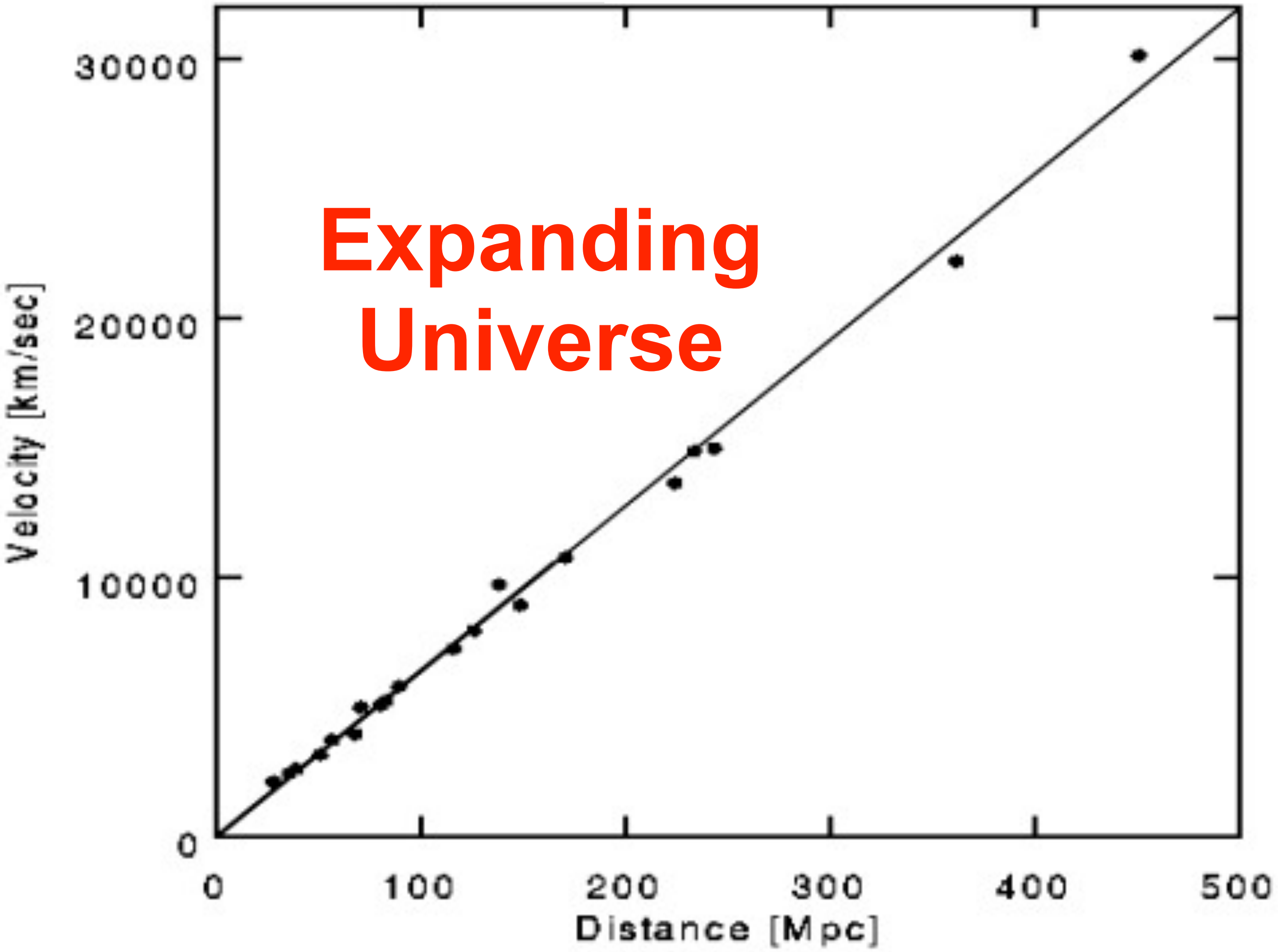

Expanding Universe

A modern illustration of Hubble's Law, displaying the increase of recession speed of galaxies growing in direct proportion to their distance.

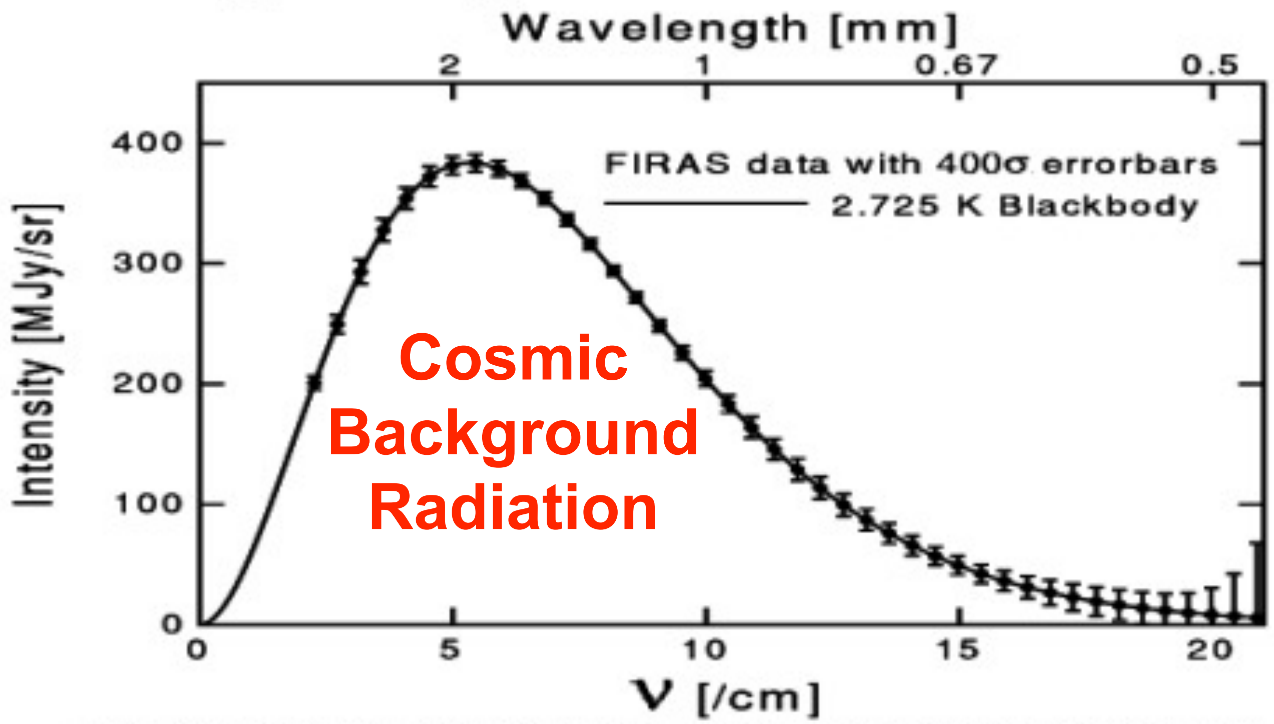

Cosmic Background Radiation

The variation of the intensity of the microwave background radiation with its frequency, as observed by the COBE satellite from above the Earth's atmosphere. The observations (boxes) display a perfect fit with the (solid) curve expected from pure heat radiation with a temperature of 2.73°K.

Big Bang Nucleosynthesis

The detailed production of the lightest elements out of protons and neutrons during the first three minutes of the universe's history. The nuclear reactions occur rapidly when the temperature falls below a billion degrees Kelvin. Subsequently, the reactions are shut down, because of the rapidly falling temperature and density of matter in the expanding universe.

Caution: ^{7}Li may now be discordant

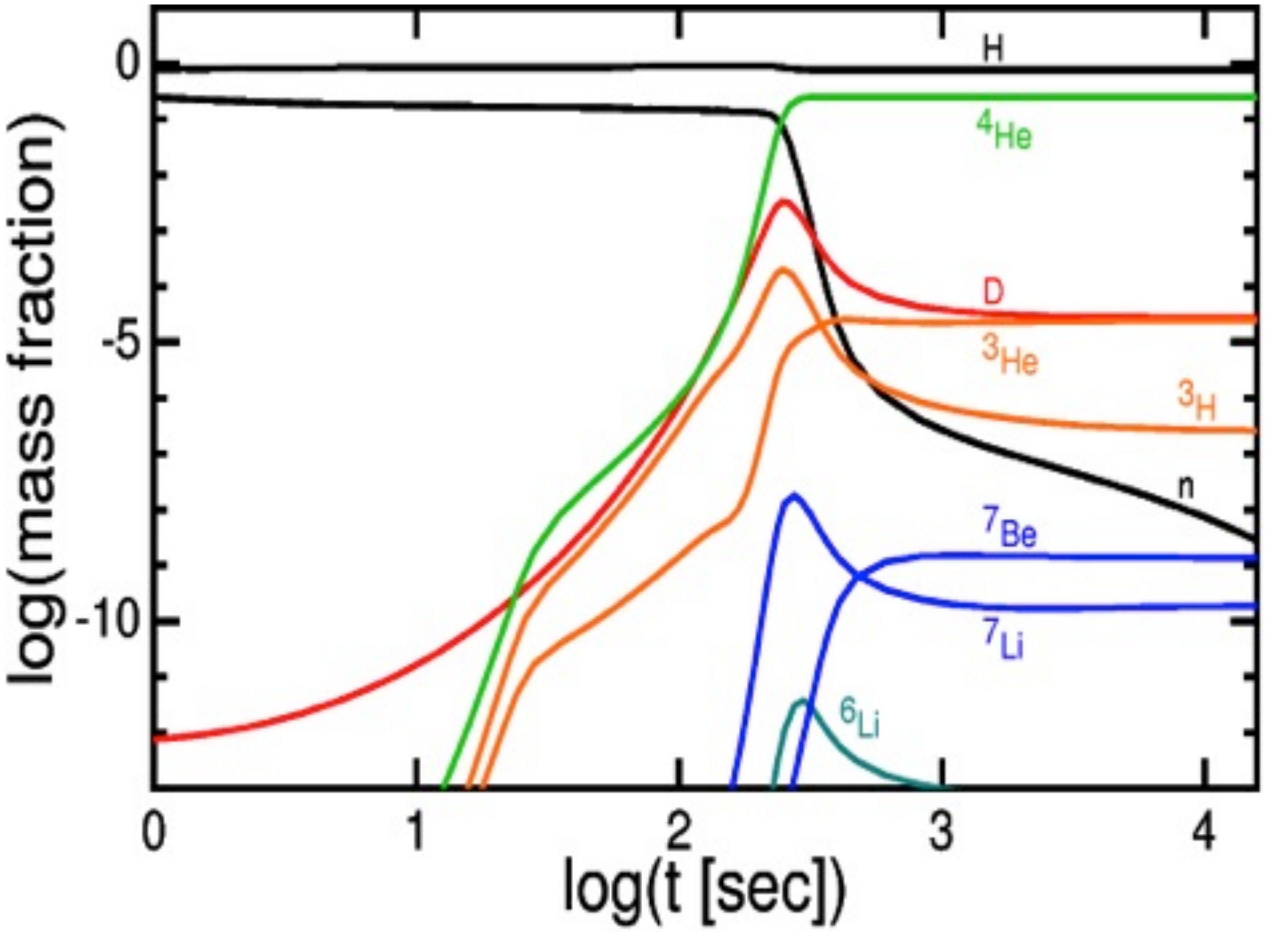

The Early Universe

In the early universe after Cosmic Inflation and until about 45,000 years, the cosmic density is dominated by relativistic particles, initially mostly massive particles having energies much greater than their masses, then just e^+, e^-, neutrinos and photons, and after a few seconds when the e+ annihilate with all but a few e^-, just the neutrinos and photons. It is therefore essential to review the densities of such particles. (See Perkins Section 5.8.)

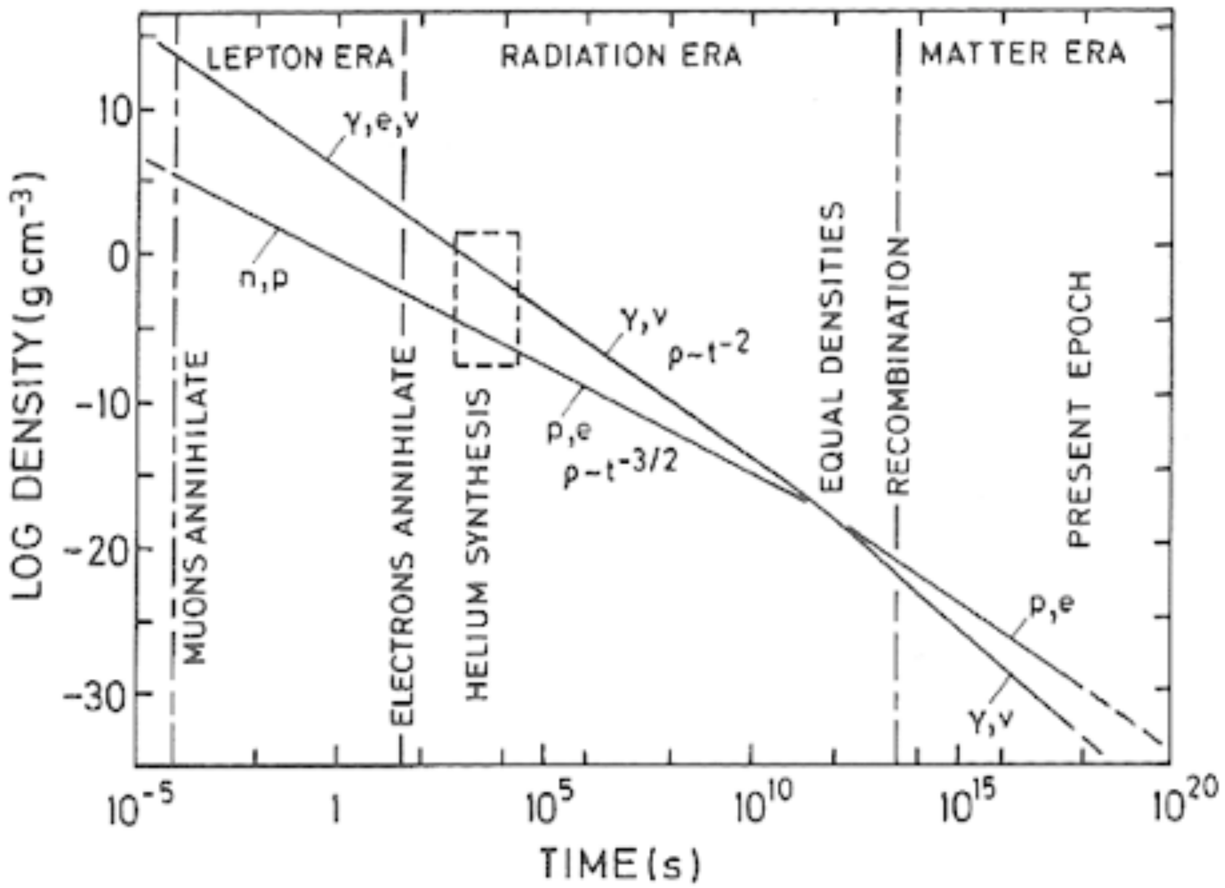

In the following slides, I summarize first the number and energy densities for the photons, and then more generally for fermions and bosons. The effective number of degrees of freedom $g^*(z)$ allows us to account for all the relativistic particles. There is an abrupt change in $g^*(z)$ at the quark-hadron phase transition at ~200 MeV. Above this temperature, quarks and gluons are free, representing a lot more possible states than just those available below ~200 MeV. Below this temperature there is an approximate time-temperature relation

$$T \approx 1 \text{ MeV } (t/\text{sec})^{-1/2} \ .$$

Thus $T = 100$ MeV corresponds roughly to $t \approx 10^{-4}$ s, and $T = 100$ keV to $t \approx 100$ s. "Freeze-out" is a key concept, describing going out of equilibrium when the relevant mean free path exceeds the Hubble length c/H.

Cosmic Radiation: Photons

Photon energy density vs. time: $\rho_r c^2 = \left(\frac{3c^2/32\pi G}{t^2}\right)$

Photon energy density vs. Temperature: $\rho_r c^2 = \frac{4\sigma T^4}{c} = \pi^4 (kT)^4 \left(\frac{g_\gamma/2}{15\pi^2\hbar^3 c^3}\right)$

Early universe Temperature (in MeV) vs. time (in seconds): $kT = \frac{\left[\left(45\hbar^3 c^5 / 16\pi^3 \mathrm{G} g_\gamma\right)^{1/4}\right]}{t^{1/2}} = 1.307 \ \frac{\mathrm{MeV}}{t^{1/2}}$

Early universe Temperature (in Kelvin) vs. time (in seconds): $T = 1.52 \times 10^{10} \frac{K}{t^{1/2}}.$

Photon (Bose-Einstein) energy distribution: $N(p)\mathrm{d}p = \frac{p^2 \mathrm{d}p}{\pi^2\hbar^3 \left\{\exp\left(E/kT\right) - 1\right\}}$

Photon number density today: $N_\gamma = \left(\frac{2.404}{\pi^2}\right)\left(\frac{kT}{\hbar c}\right)^3 = 411\left(\frac{T}{2.725}\right)^3 = 411 \ \ \mathrm{cm}^{-3}$

$$N_\gamma = \frac{2\zeta(3)}{\pi^2} T^3 \ \text{ with } \ 2\zeta(3)/\pi^2 \simeq 0.2436.$$

Photon energy density today: $\rho_r c^2 = 0.261 \ \ \mathrm{MeV\,m^{-3}}$ or $\Omega_\gamma(0) = 4.84 \times 10^{-5}$

Particles and Radiation in the Early Universe

Fermi-Dirac energy distribution:

$$N(p)\mathrm{d}p = \frac{p^2\mathrm{d}p}{\pi^2\hbar^3\left\{\exp\left(E/kT\right)+1\right\}}\left(\frac{g_f}{2}\right)$$

Here $E^2=p^2+m^2$, and
g_f = number of spin states

Using these integrals one can find the energy and entropy densities for B-E and F-D distributions:

$$\mathrm{BE}: \quad \int\frac{x^3\mathrm{d}x}{(e^x-1)} = \frac{\pi^4}{15}; \quad \int\frac{x^2\mathrm{d}x}{(e^x-1)} = 2.404$$

$$\mathrm{FD}: \quad \int\frac{x^3\mathrm{d}x}{(e^x+1)} = \frac{7}{8}\times\frac{\pi^4}{15}; \quad \int\frac{x^2\mathrm{d}x}{(e^x+1)} = \frac{3}{4}\times 2.404$$

For the F-D distribution, the result for highly relativistic particles ($kT >> m$) is

$$\rho_f c^2 = \left(\frac{7}{8}\right)\pi^4(kT)^4\frac{(g_f/2)}{15\pi^2\hbar^3c^3}$$

For the B-E distribution, the result for photons ($g_\gamma = 2$) is

$$\rho_r c^2 = \frac{4\sigma T^4}{c} = \pi^4(kT)^4\left(\frac{g_\gamma/2}{15\pi^2\hbar^3c^3}\right)$$

For a mixture of highly relativistic fermions and bosons, replace g_γ by g^* including bosons and fermions

$$g^* = \sum g_b + \left(\frac{7}{8}\right)\sum g_f$$

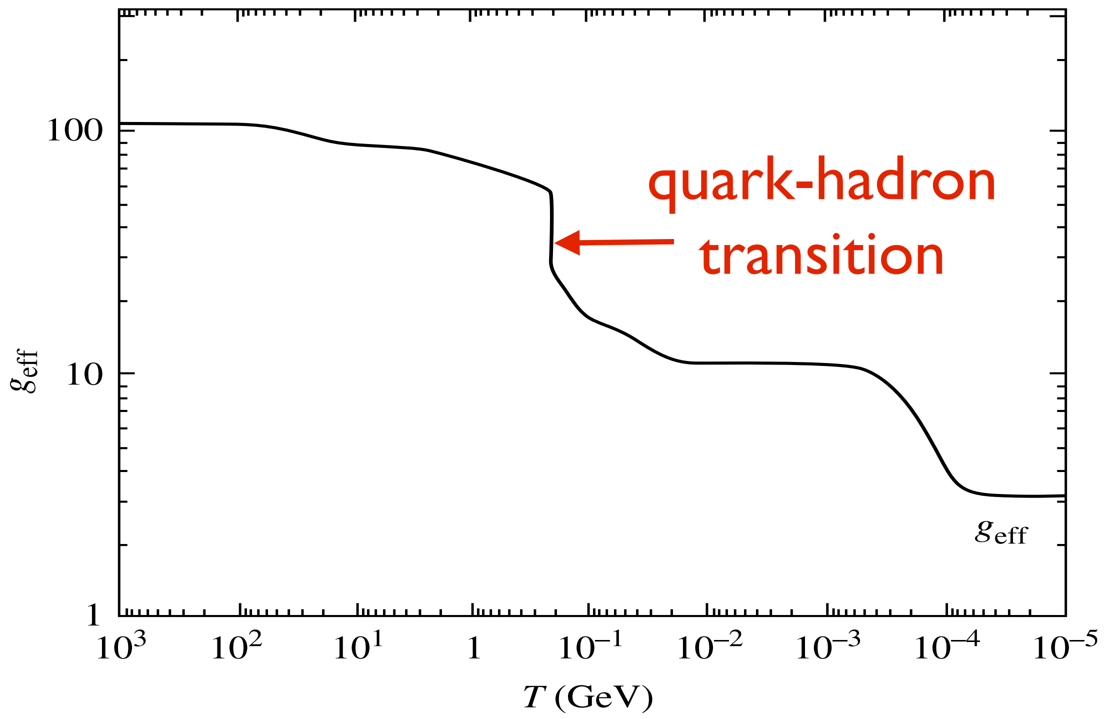

quark-hadron transition

Perkins Fig. 5.9

Particles and Radiation in the Early Universe

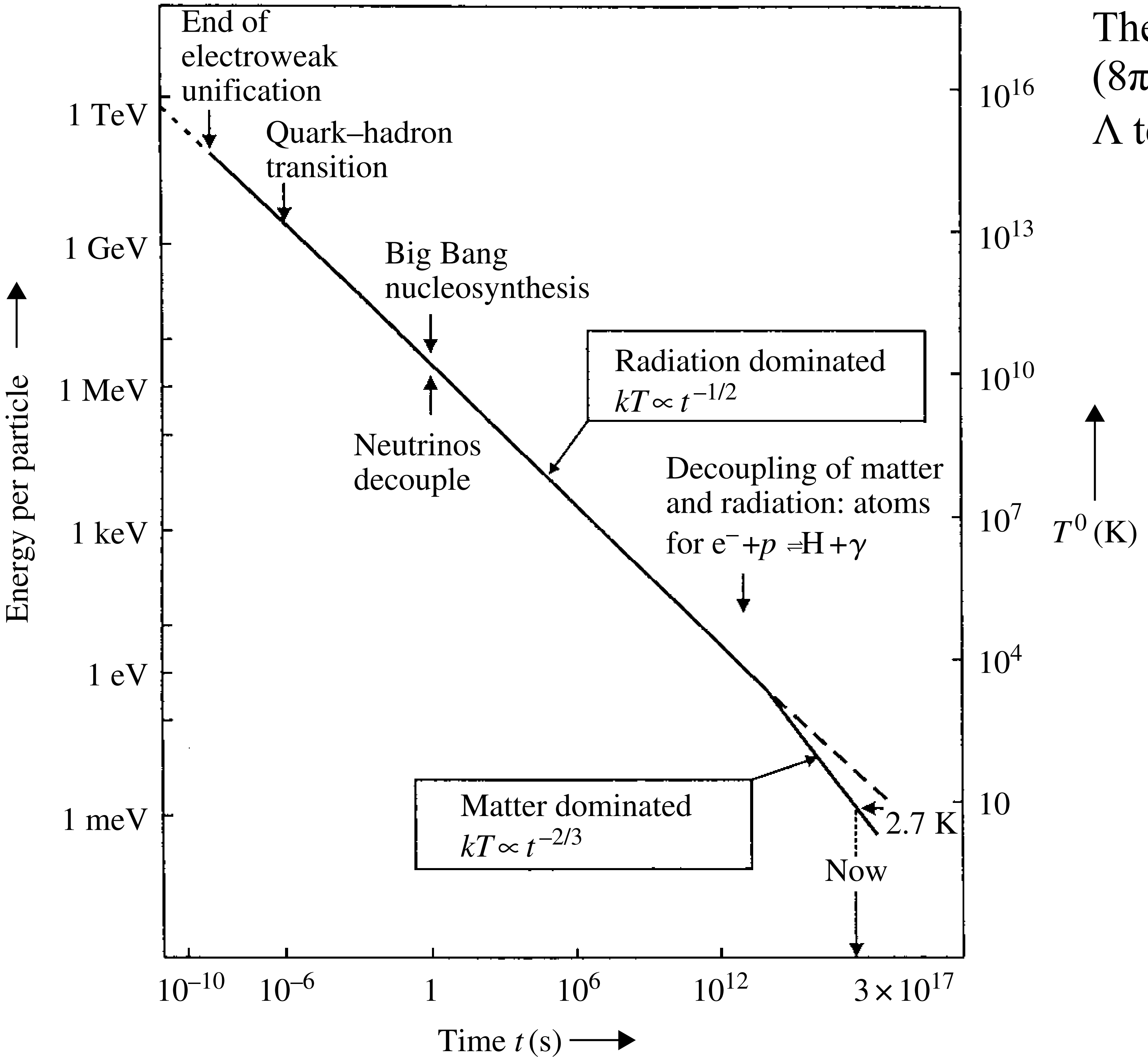

The Friedmann equation says that $H^2 = (8\pi G/3)\,\rho$ in the early universe, where the Λ term is negligible and $\rho \propto g^* T^4$, so

$$H(t) = \left[\frac{4g^*\pi^3 G}{45\hbar^3 c^5}\right]^{1/2} (kT)^2$$

$$= \frac{(4\pi^3 g^*/45)^{1/2}}{M_{PL}\hbar c^2} \times (kT)^2$$

$$= 1.66 g^{*1/2} \frac{(kT)^2}{M_{PL}\hbar c^2}$$

Here G was replaced by the Planck mass $M_{PL} = \left(\frac{\hbar c}{G}\right)^{1/2} = 1.2 \times 10^{19}\ \frac{\text{GeV}}{c^2}$

Big Bang Nucleosynthesis

The synthesis of the light elements is sensitive to physical conditions in the early radiation-dominated era at a temperature T ~ 1 MeV, corresponding to an age t ~ 1 s. At higher temperatures, weak interactions were in thermal equilibrium, thus fixing the ratio of the neutron and proton number densities to be $n/p = e^{-Q/T}$, where Q = 1.293 MeV is the neutron-proton mass difference. As the temperature dropped, the neutron-proton inter-conversion rate per nucleon, $\Gamma_{n\leftrightarrow p} \sim G_F{}^2T^5$, fell faster than the Hubble expansion rate, $H \sim T^2\sqrt{g_*}$, where g_* counts the number of relativistic particle species determining the energy density in radiation. This resulted in departure from chemical equilibrium ('freeze-out') at $T_{fr} \sim 1$ MeV. The neutron fraction at this time, $n/p = \exp(-Q/T_{fr}) \simeq 1/6$, is thus sensitive to every known physical interaction, since Q is determined by both strong and electromagnetic interactions while T_{fr} depends on the weak as well as gravitational interactions. Moreover, the sensitivity to the Hubble expansion rate affords a probe of, e.g., the number of relativistic neutrino species. After freeze-out, the neutrons were free to β-decay, so the neutron fraction dropped to $n/p \simeq 1/7$ by the time nuclear reactions began, locking up almost all the n in ^{4}He.

http://pdg.lbl.gov/2013/reviews/rpp2013-rev-bbang-nucleosynthesis.pdf

Big Bang Nucleosynthesis

BBN was conceived by Gamow in 1946 as an explanation for the formation of all the elements, but the absence of any stable nuclei with A=5,8 makes it impossible for BBN to proceed past Li. The formation of carbon and heavier elements occurs instead through the triple-α process in the centers of red giants (Burbidge^2, Fowler, & Hoyle 1957). At the BBN baryon density of $2\times10^{-29}\ \Omega_b\ h^2\ (T/T_0)^3$ g cm^{-3} $\approx 2\times10^{-5}$ g cm^{-3}, the probability of the triple-α process is negligible even though $T \approx 10^9$K.

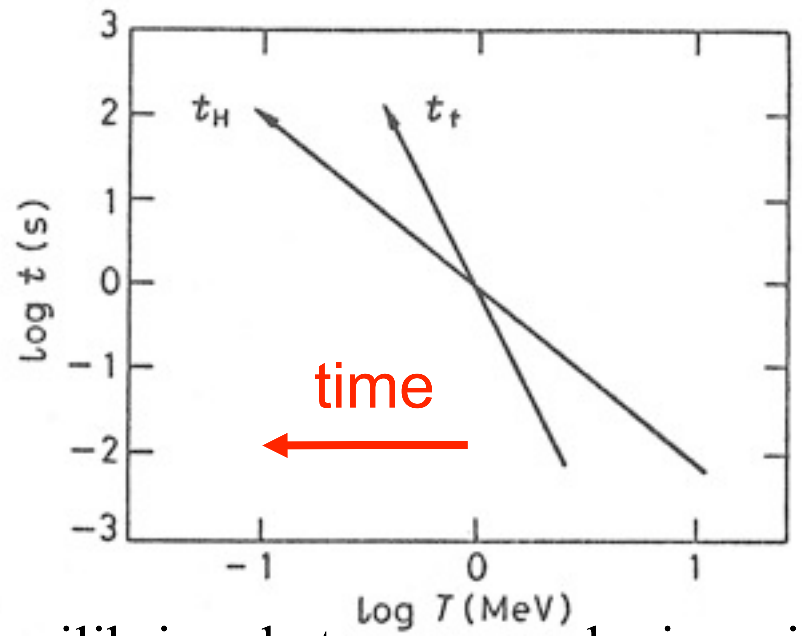

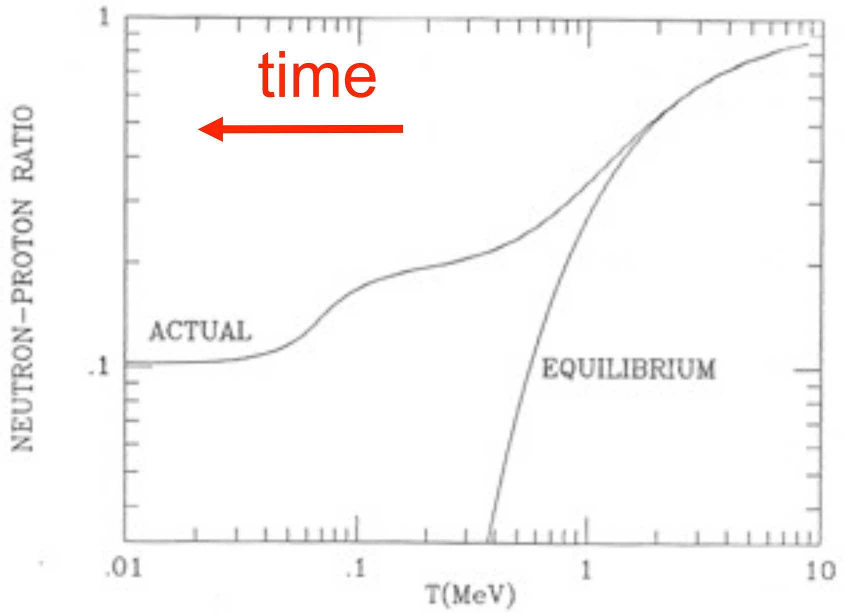

Kolb & Turner

Thermal equilibrium between n and p is maintained by weak interactions, which keeps n/p = exp(-Q/T) (where $Q = m_n - m_p = 1.293$ MeV) until about t ≈ 1 s. But because the neutrino mean free time $t_\nu^{-1} \approx \sigma_\nu\, n_{e\pm} \approx (G_F T)^2 (T^3)$ is increasing as $t_\nu \propto T^{-5}$ (recall that the Fermi constant $G_F \approx 10^{-5}$ GeV^{-2}), while the horizon size is increasing only as $t_H \approx (G\rho)^{-½} \approx M_{Pl}\, T^{-2}$, these interactions **freeze out** when T drops below about 0.8 MeV. This leaves n/(p+n) ≈ 0.14. The neutrons then decay with a mean lifetime 887 ± 2 s until they are mostly fused into D and then ^{4}He. The higher the baryon density, the higher the final abundance of ^{4}He and the lower the abundance of D that survives this fusion process. Since D/H is so sensitive to baryon density, David Schramm called deuterium the "baryometer." He and his colleagues also pointed out that since the horizon size increases more slowly with T^{-1} the larger the number of light neutrino species N_ν contributing to the energy density ρ, BBN predicted that $N_\nu \approx 3$ before N_ν was measured at accelerators by measuring the width of the Z^0 (Cyburt et al. 2005: $2.67 < N_\nu < 3.85$; Current limit: $N_\nu = 2.984 \pm 0.008$).

Neutrinos in the Early Universe

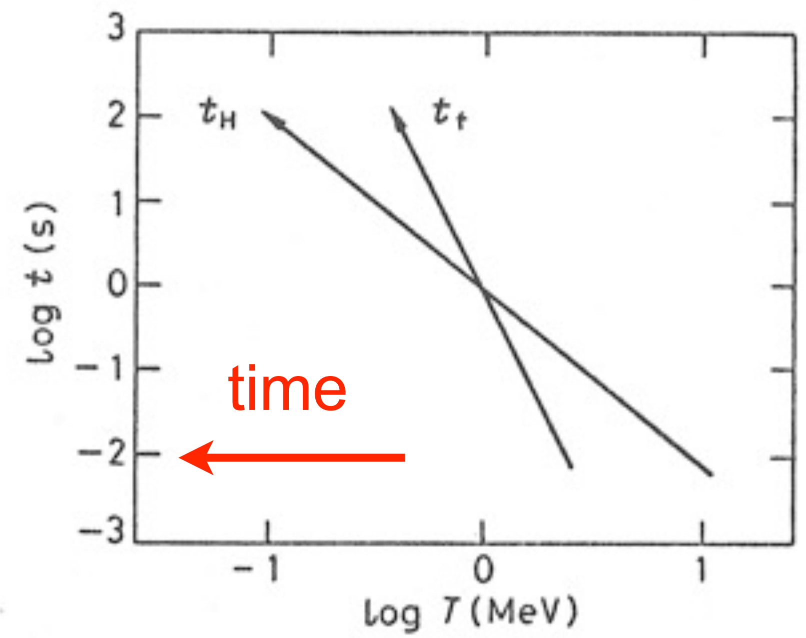

As we discussed, neutrino decoupling occurs at T ~ 1 MeV. After decoupling, the neutrino phase space distribution is

$f_\nu = [1+\exp(p_\nu c/T_\nu)]^{-1}$ $\Big($note: $\neq [1+\exp(E_\nu/T_\nu)]^{-1}$ for NR neutrinos$\Big)$

After e+e- annihilation, $T_\nu=(4/11)^{1/3}T_\gamma = 1.95$K.

Number densities of primordial particles

FermiDirac/BoseEinstein factor

$n_\gamma(T) = 2\,\zeta(3)\,\pi^{-2}\,T^3 = 411\text{ cm}^{-3}\,(T/2.725\text{K})^3$, $n_\nu(T) = (3/4)\,n_\gamma(T)$ including antineutrinos

Conservation of entropy s_I of interacting particles per comoving volume

$s_I = g_I(T)\,N_\gamma(T)$ = constant, where $N_\gamma = n_\gamma V$; we only include neutrinos for T>1 MeV.

Thus for T>1 MeV, $g_I = 2 + 4(7/8) + 6(7/8) = 43/4$ for γ, e+e-, and the three ν species, while for T< 1 MeV, $g_I = 2 + 4(7/8) = 11/2$. At e+e- annihilation, below about T=0.5 Mev, g_I drops to 2, so that $2N_{\gamma 0} = g_I(T<1\text{ MeV})\,N_\gamma(T<1\text{ MeV}) = (11/2)\,N_\gamma(T<1\text{ MeV}) = (11/2)(4/3)\,N_\nu(T<1\text{ MeV})$. Thus $n_{\nu 0} = (3/4)(4/11)\,n_{\gamma 0} = 113\text{ cm}^{-3}\,(T/2.725\text{K})^3$, or

$T_\nu = (4/11)^{1/3}\,T_\gamma = 0.714\,T_\gamma = 1.95\text{K}\,(T_\gamma/2.725\text{K})$

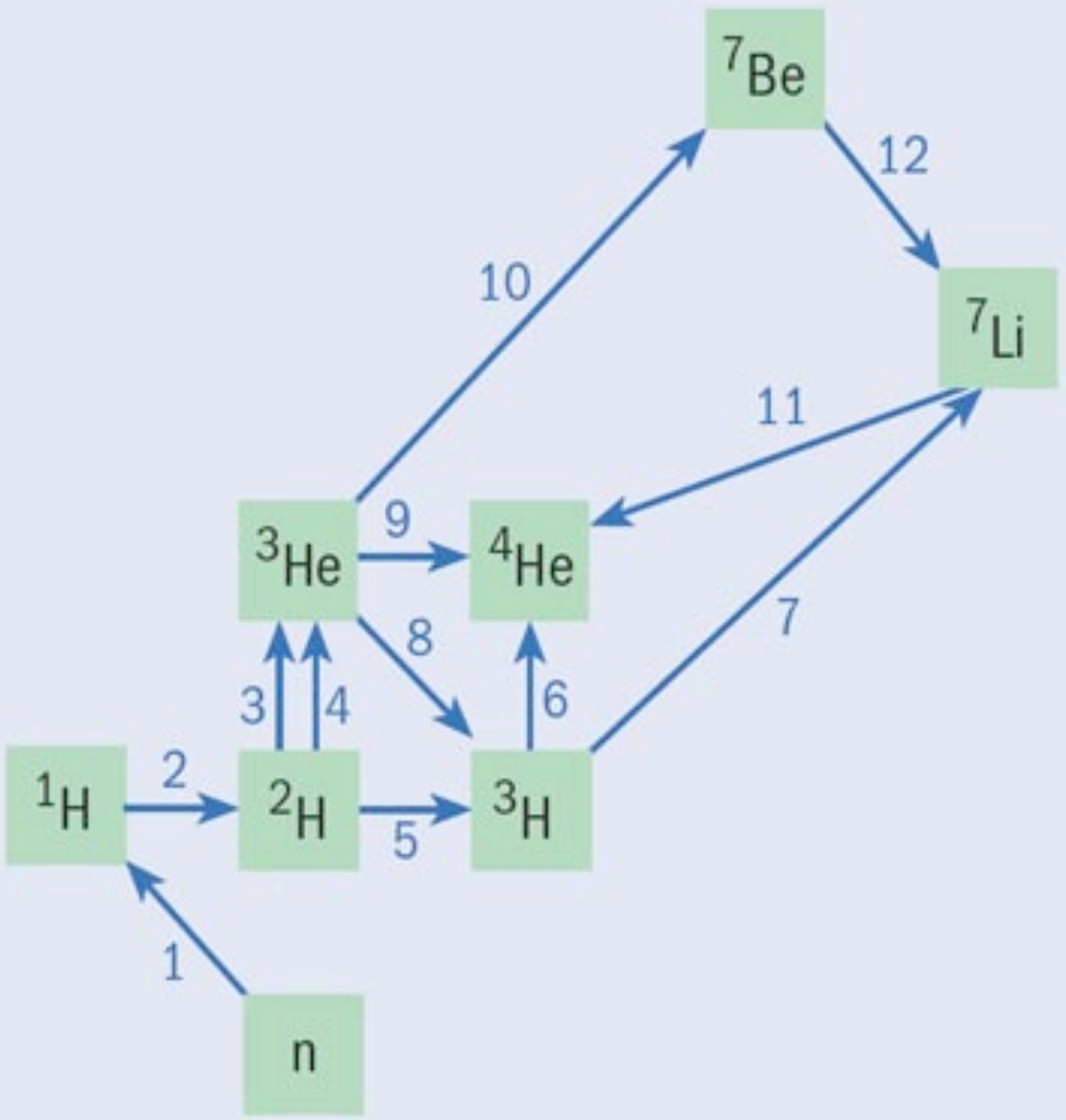

1 $n \rightarrow {}^{1}H + e^{-} + \bar{\nu}$

2 ${}^{1}H + n \rightarrow {}^{2}H + \gamma$

3 ${}^{2}H + {}^{1}H \rightarrow {}^{3}He + \gamma$

4 ${}^{2}H + {}^{2}H \rightarrow {}^{3}He + n$

5 ${}^{2}H + {}^{2}H \rightarrow {}^{3}H + {}^{1}H$

6 ${}^{2}H + {}^{3}H \rightarrow {}^{4}He + n$

7 ${}^{3}H + {}^{4}He \rightarrow {}^{7}Li + \gamma$

8 ${}^{3}He + n \rightarrow {}^{3}H + {}^{1}H$

9 ${}^{3}He + {}^{2}H \rightarrow {}^{4}He + {}^{1}H$

10 ${}^{3}He + {}^{4}He \rightarrow {}^{7}Be + \gamma$

11 ${}^{7}Li + {}^{1}H \rightarrow {}^{4}He + {}^{4}He$

12 ${}^{7}Be + n \rightarrow {}^{7}Li + {}^{1}H$

Deuterium nuclei (^{2}H) were produced by collisions between protons and neutrons, and further nuclear collisions led to every neutron grabbing a proton to form the most tightly bound type of light nucleus: ^{4}He. This process was complete after about five minutes, when the universe became too cold for nuclear reactions to continue. Tiny amounts of deuterium, ^{3}He, ^{7}Li, and ^{7}Be were produced as by-products, with the ^{7}Be undergoing beta decay to form ^{7}Li. Almost all of the protons that were not incorporated into ^{4}He nuclei remained as free particles, and this is why the universe is close to 25% ^{4}He and 75% H by mass. The other nuclei are less abundant by several orders of magnitude.

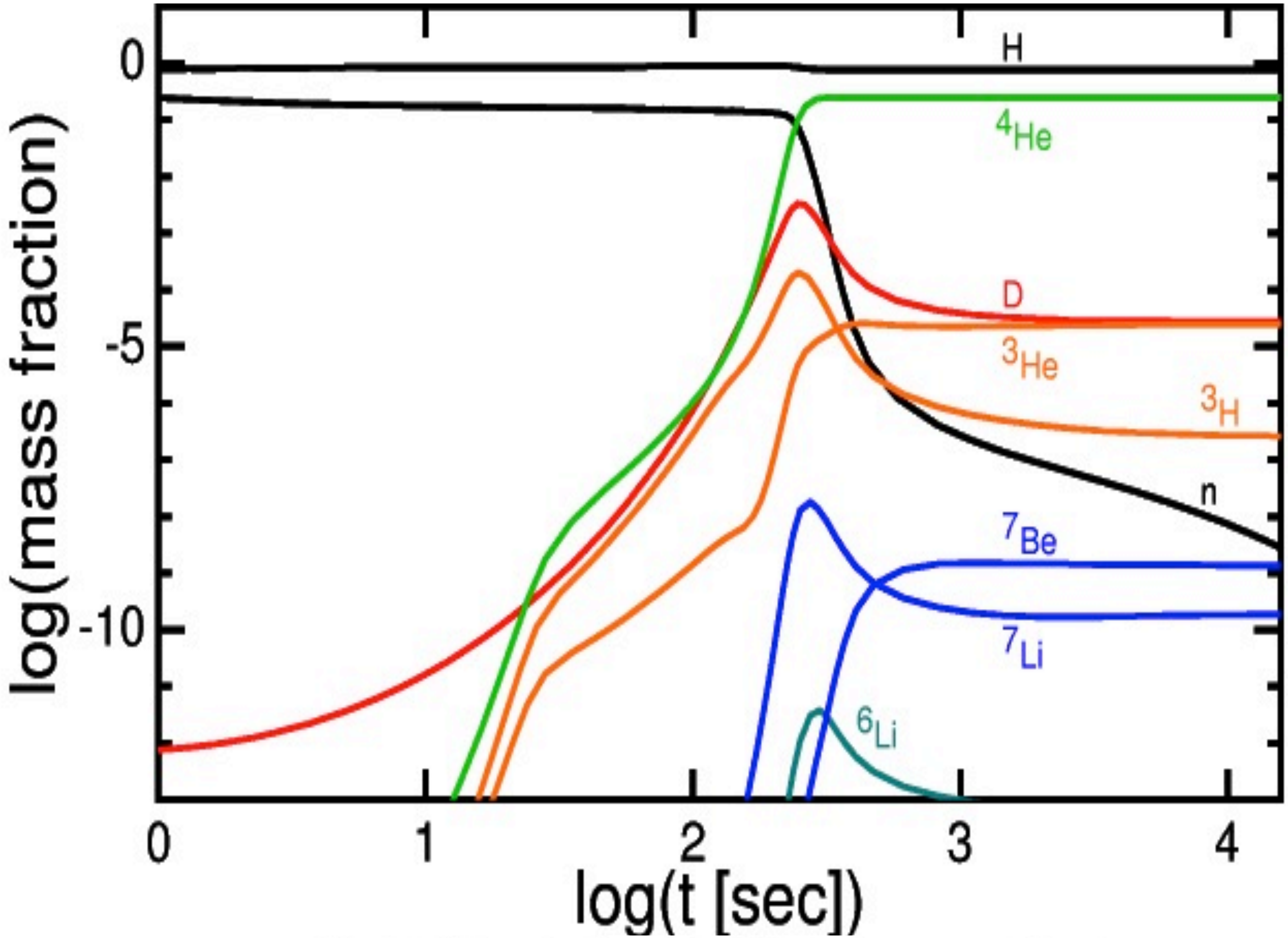

The detailed production of the lightest elements out of protons and neutrons during the first three minutes of the universe's history. The nuclear reactions occur rapidly when the temperature falls below a billion degrees Kelvin. Subsequently, the reactions are shut down, because of the rapidly falling temperature and density of matter in the expanding universe.

Ken Kawano's (1992) BBN code is available at
http://www-thphys.physics.ox.ac.uk/users/SubirSarkar/bbn.html

The abundances of ^{4}He, D, ^{3}He, and ^{7}Li as predicted by the standard model of Big-Bang nucleosynthesis — the bands show the 95% CL range. Boxes indicate the observed light element abundances. The narrow vertical band indicates the CMB measure of the cosmic baryon density, while the wider band indicates the BBN concordance range (both at 95% CL). (From PDG BBN Review, 2013.)

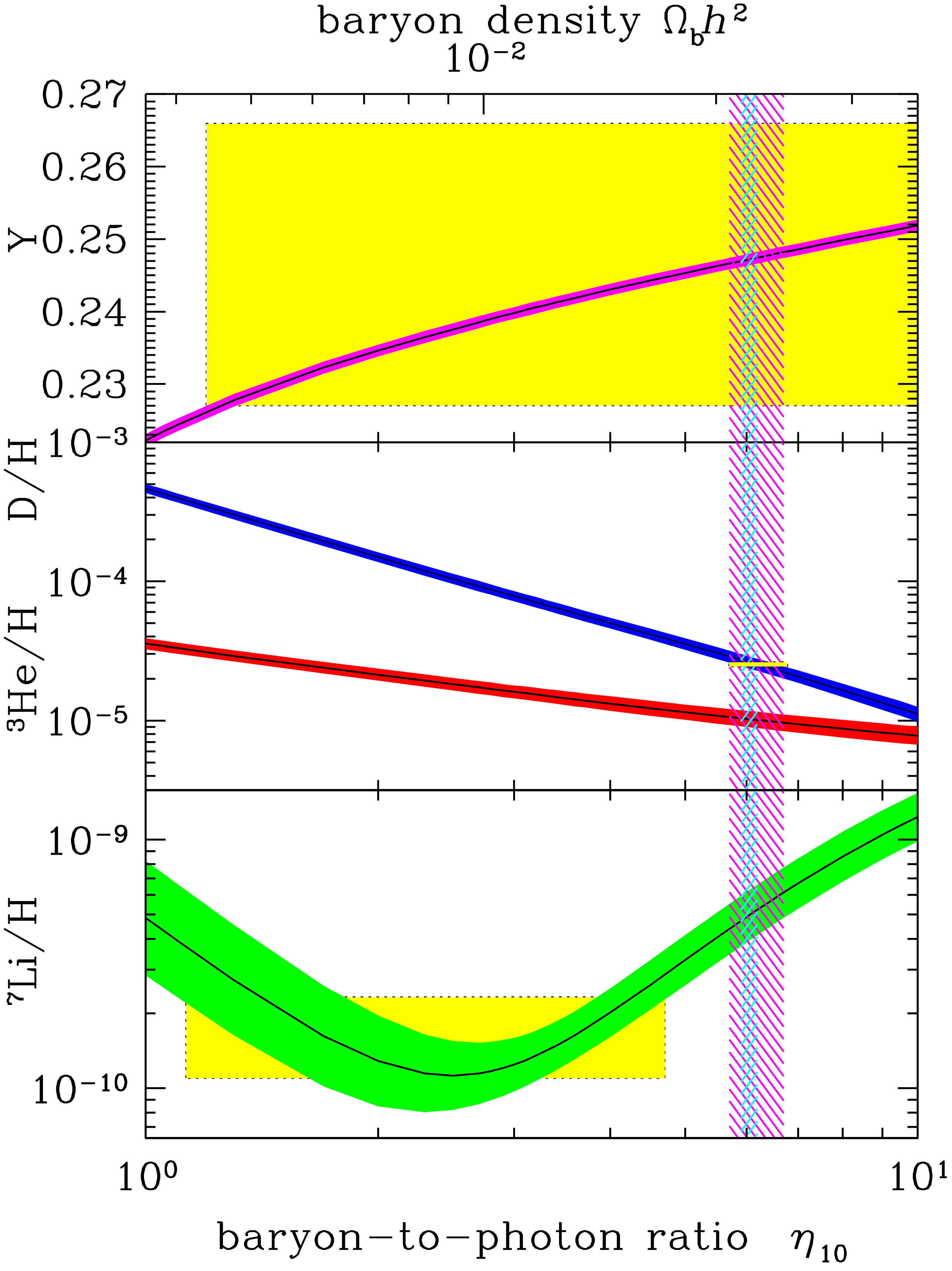

^{7}Li observations are now discordant, but it has been suggested that ^{7}Li is depleted in the stars used to measure it or else perhaps in the early universe.

5 INDEPENDENT MEASURES AGREE: ATOMS ARE ~4.5% OF THE COSMIC DENSITY

Galaxy Cluster in X-rays

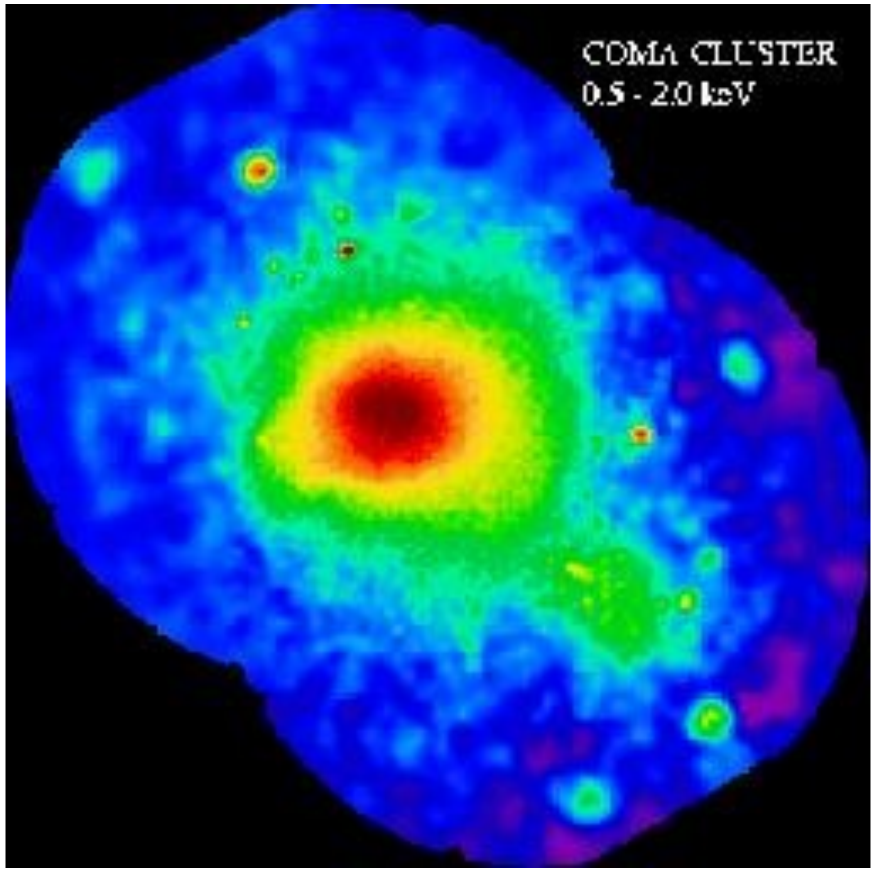

Absorption of Quasar Light

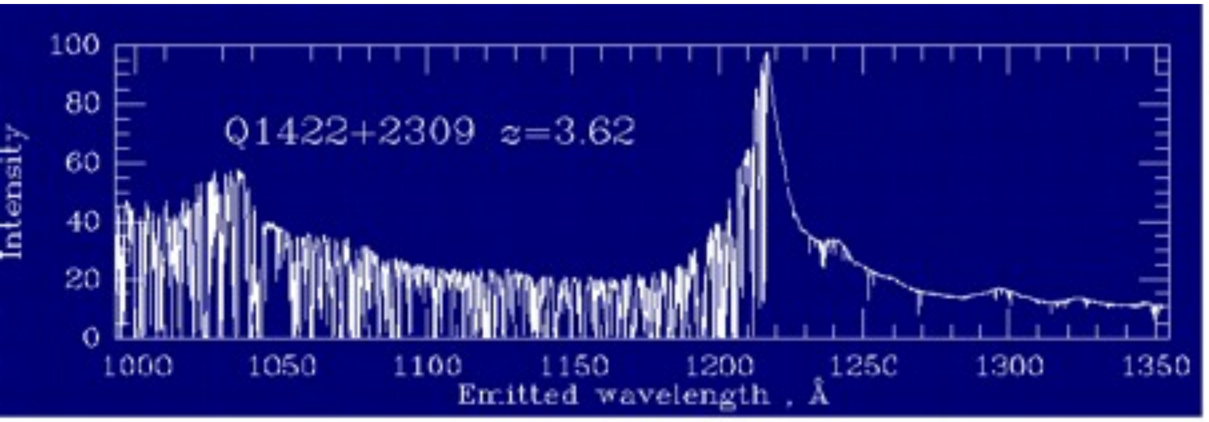

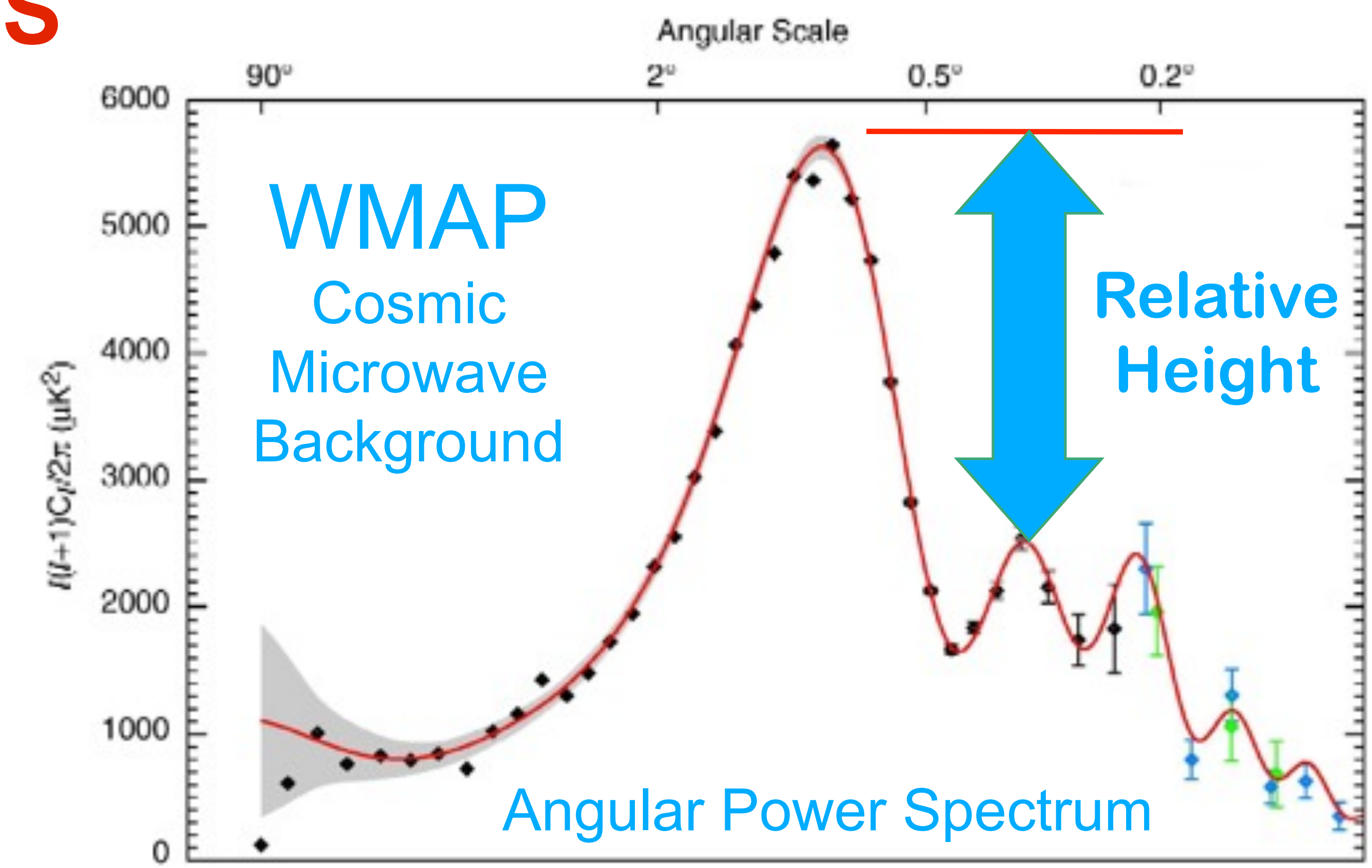

WMAP
Cosmic
Microwave
Background

Angular Power Spectrum

Deuterium Abundance
+ Big Bang Nucleosynthesis

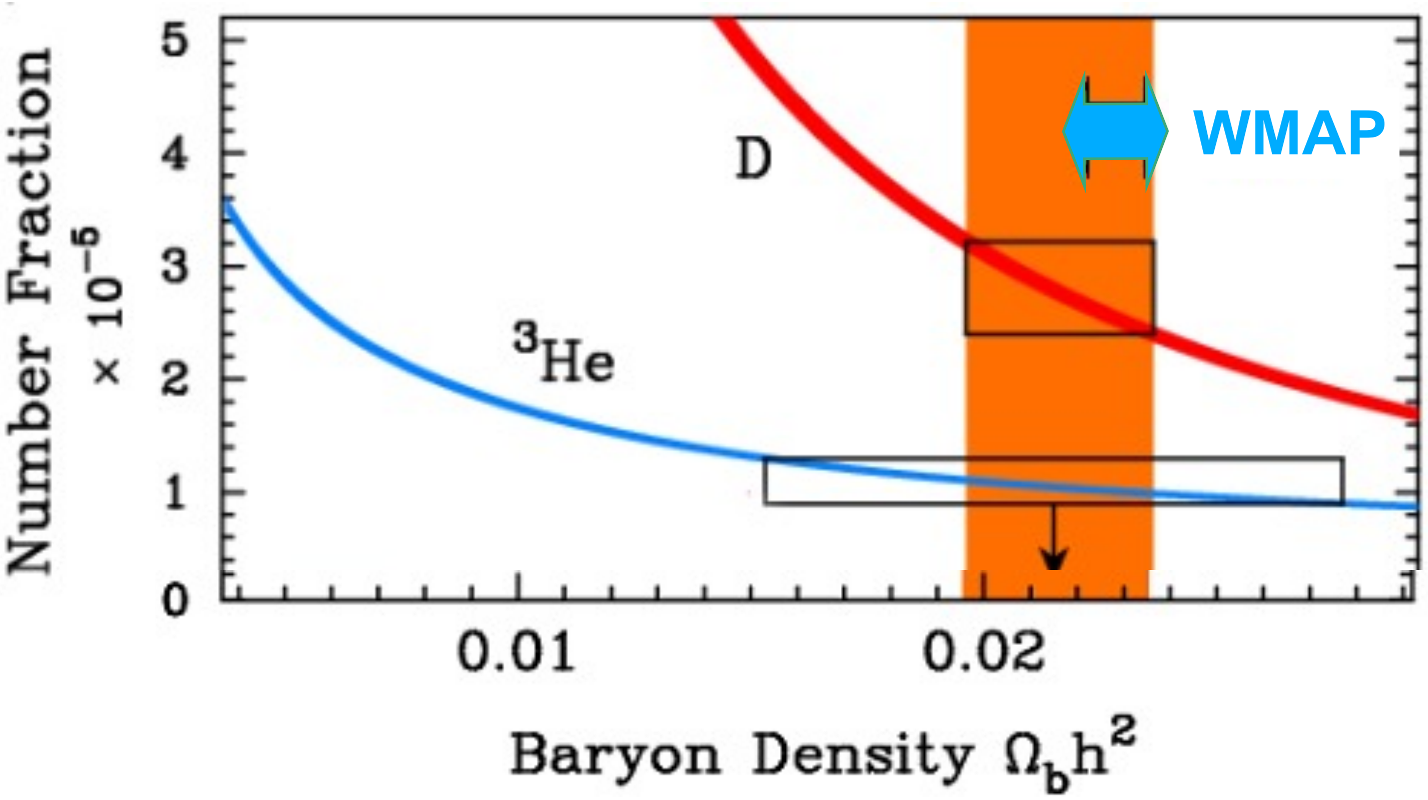

& WIGGLES IN GALAXY P(k)

BAO WIGGLES IN GALAXY P(k)

Sound waves that propagate in the opaque early universe imprint a characteristic scale in the clustering of matter, providing a “standard ruler” whose length can be computed using straightforward physics and parameters that are tightly constrained by CMB observations. Measuring the angle subtended by this scale determines a distance to that redshift and constrains the expansion rate.

The detection of the acoustic oscillation scale is one of the key accomplishments of the SDSS, and even this moderate signal-to-noise measurement substantially tightens constraints on cosmological parameters. Observing the evolution of the BAO standard ruler provides one of the best ways to measure whether the dark energy parameters changed in the past.

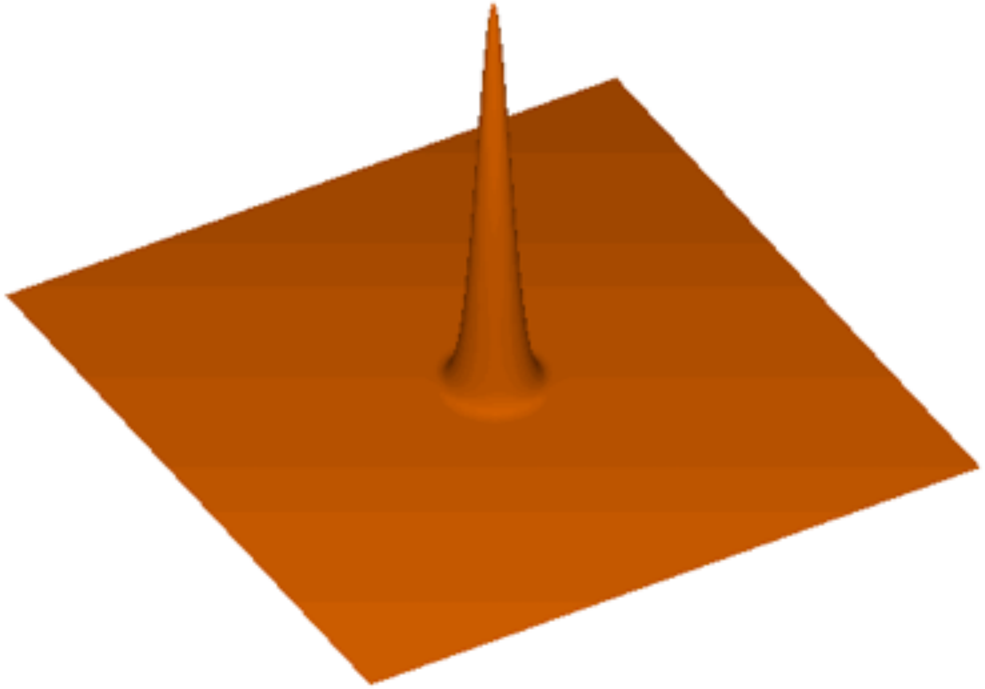

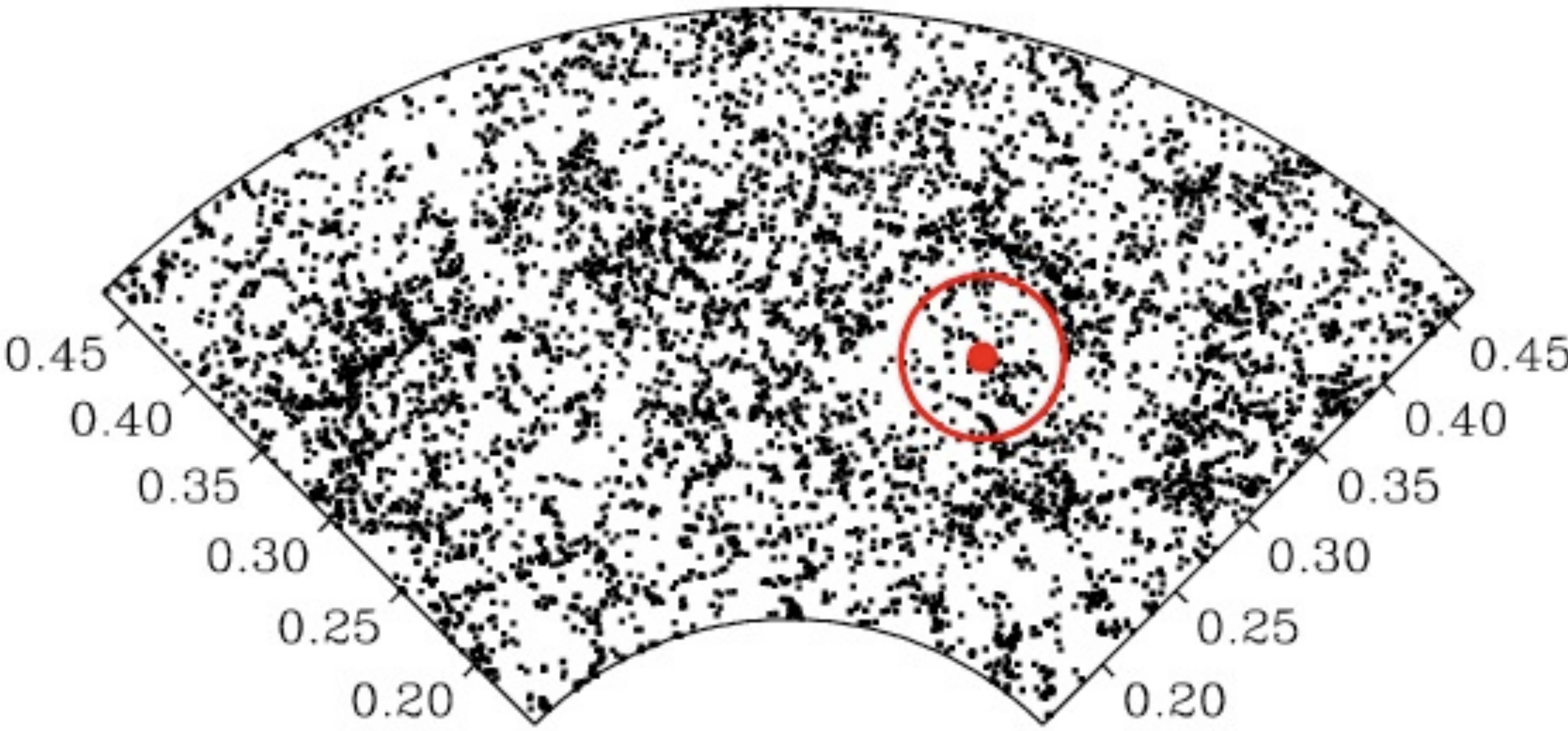

M. White lectures 08

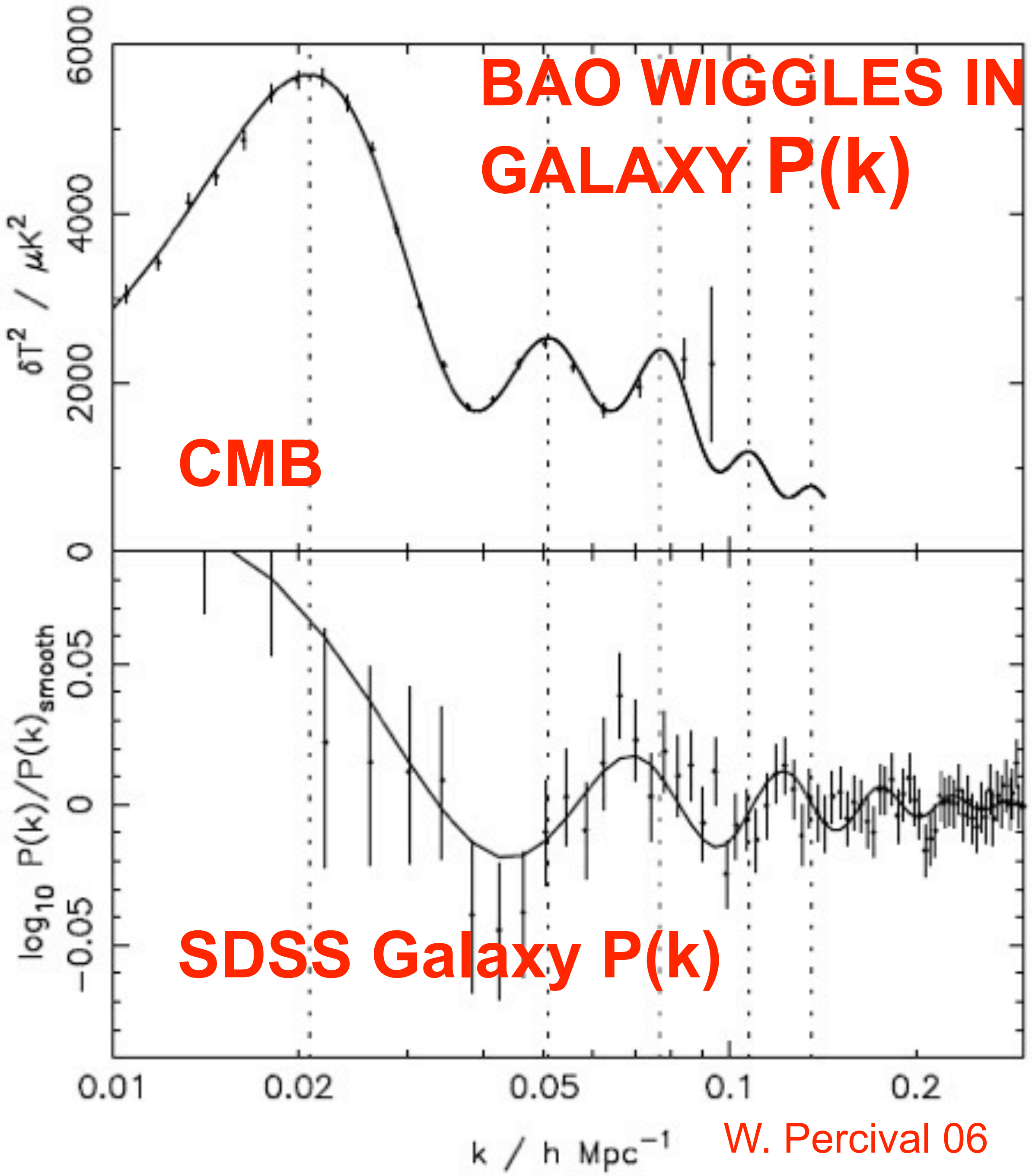

BAO WIGGLES IN GALAXY P(k)

CMB

SDSS Galaxy P(k)

W. Percival 06

Fig. 3. Upper panel: The TT power spectrum recovered from the 3-year WMAP data (Hinshaw et al. 2006), projected into comoving space assuming a cosmological model with $\Omega_m = 0.25$ and $\Omega_V = 0.75$. For comparison, in the lower panel we plot the baryon oscillations calculated by dividing the SDSS power spectrum with a smooth cubic spline fit (Percival et al. 2007a). Vertical dotted lines show the positions of the peaks in the CMB power spectrum. As can be seen, there is still a long way to go before low redshift observations can rival the CMB in terms of the significance of the acoustic oscillation signal.

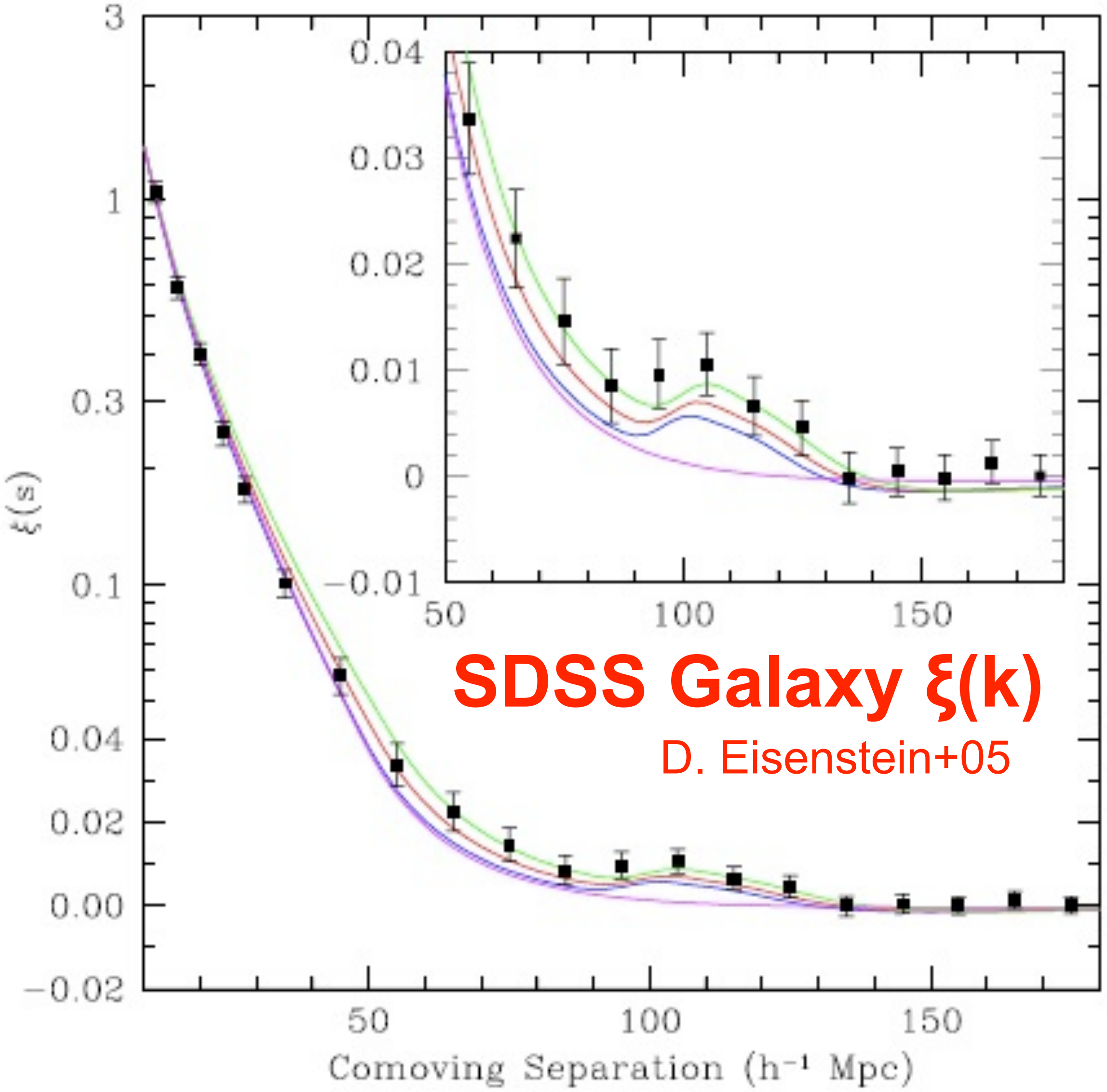

SDSS Galaxy ξ(k)

D. Eisenstein+05

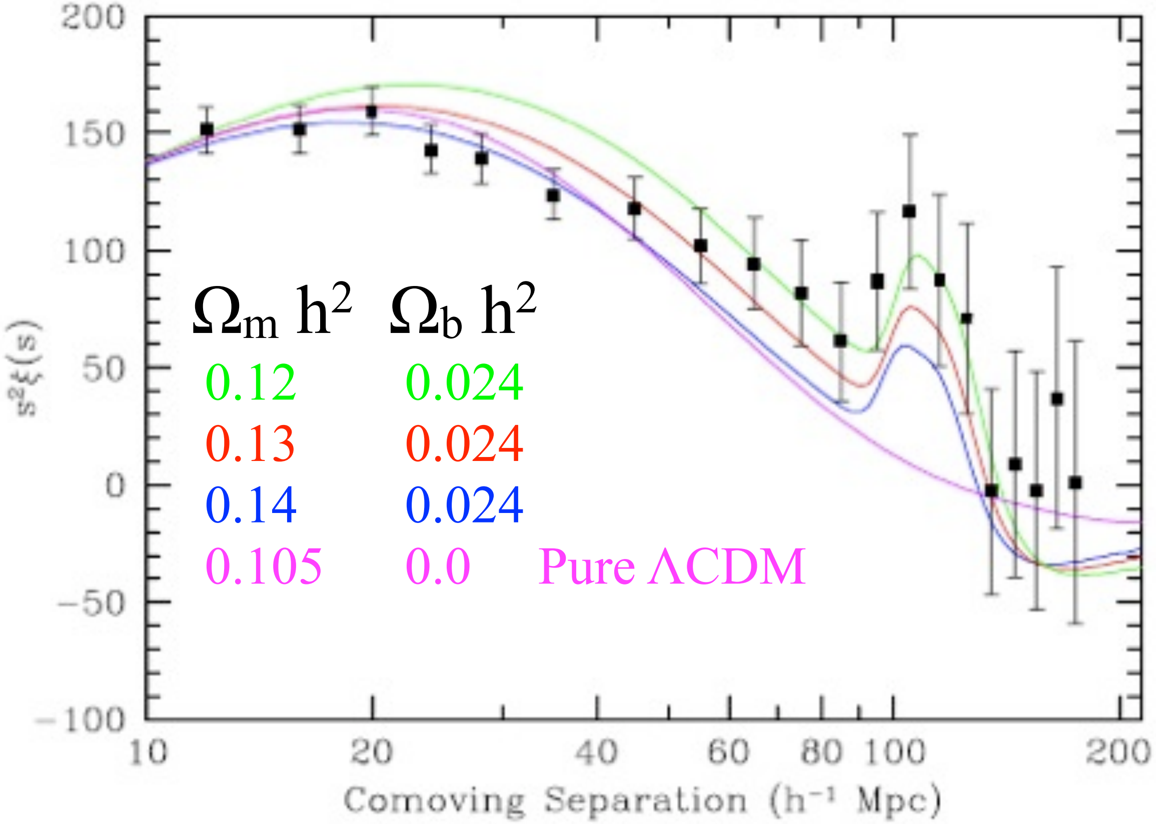

$\Omega_m h^2$	$\Omega_b h^2$	
0.12	0.024	
0.13	0.024	
0.14	0.024	
0.105	0.0	Pure ΛCDM

BOSS DR10-11 BAO data (Anderson+ arXiv: 1312.4877)

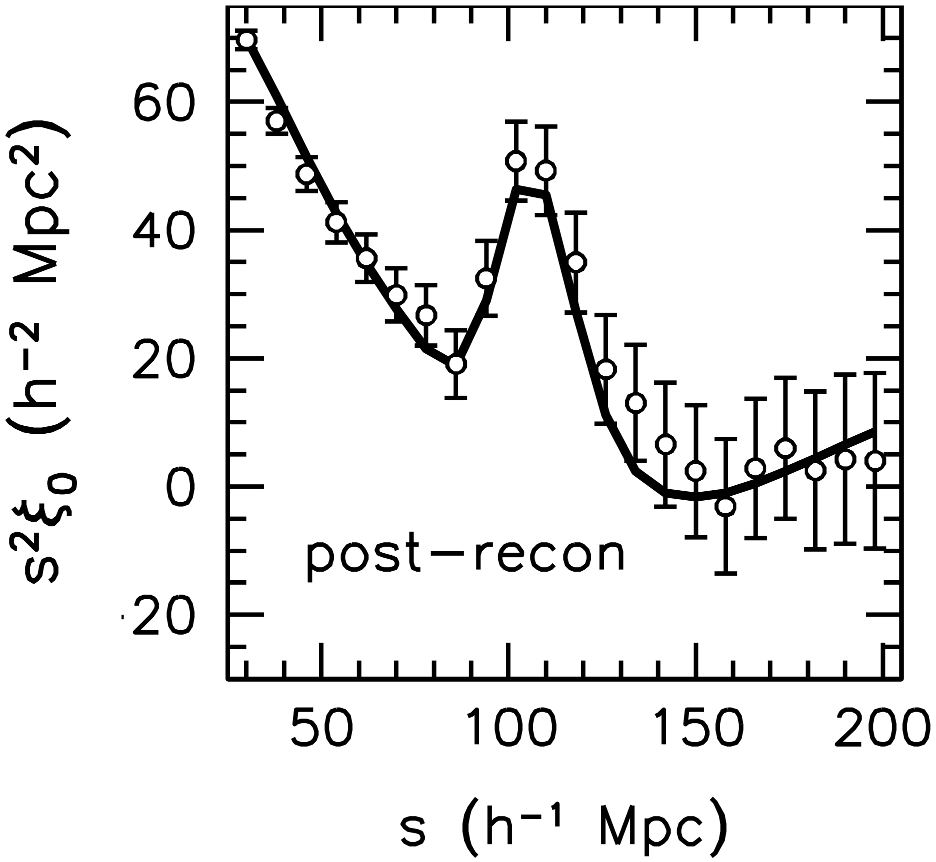

We present a one per cent measurement of the cosmic distance scale from the detections of the baryon acoustic oscillations in the clustering of galaxies from the Baryon Oscillation Spec- troscopic Survey (BOSS), which is part of the Sloan Digital Sky Survey III (SDSS-III). Our results come from the Data Release 11 (DR11) sample, containing nearly one million galax- ies and covering approximately 8 500 square degrees and the redshift range 0.2 < z < 0.7. ... Our measurements of the distance scale are in good agreement with previous BAO measurements and with the predictions from cosmic mi- crowave background data for a spatially flat cold dark matter model with a cosmological constant.

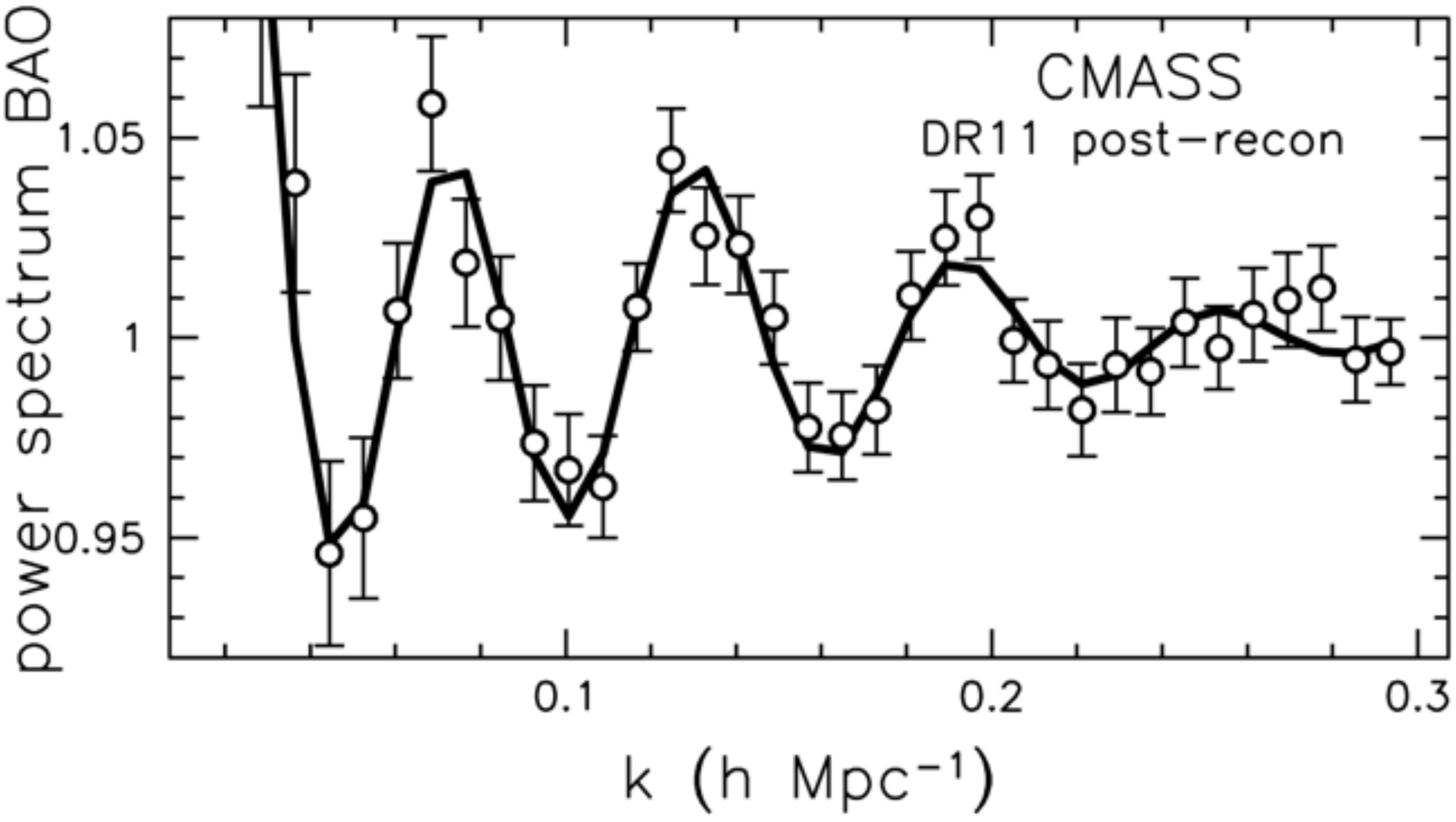

Determination of primordial He^4 abundance Y_p by linear regression

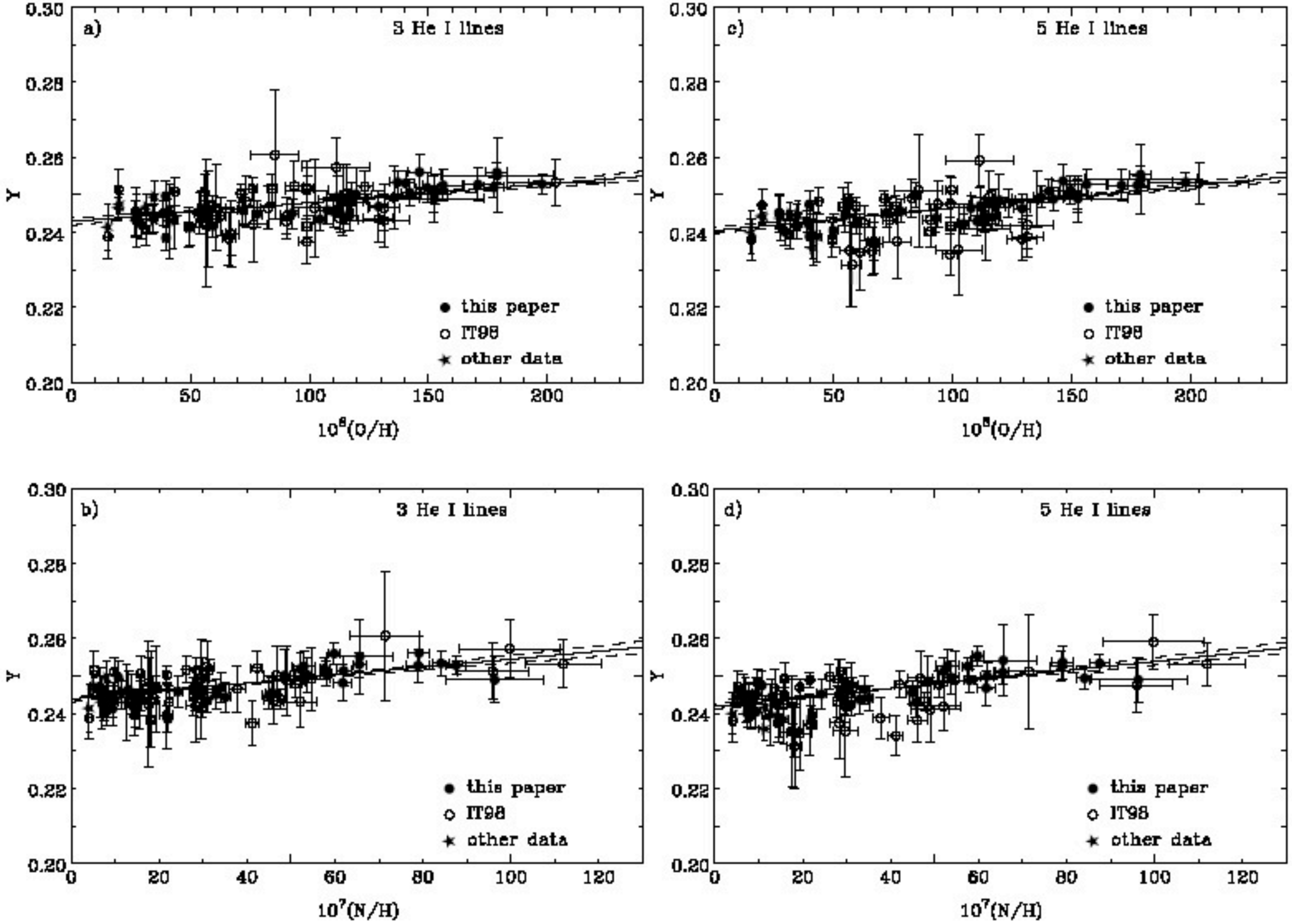

Y = M(^{4}He)/M(baryons), Primordial Y ≡ Yp = zero intercept

Note: BBN plus D/H ⇒ Yp = 0.247± 0.001

Izotov & Thuan 2004

Deuterium absorption at redshift 2.525659 towards Q1243+3047

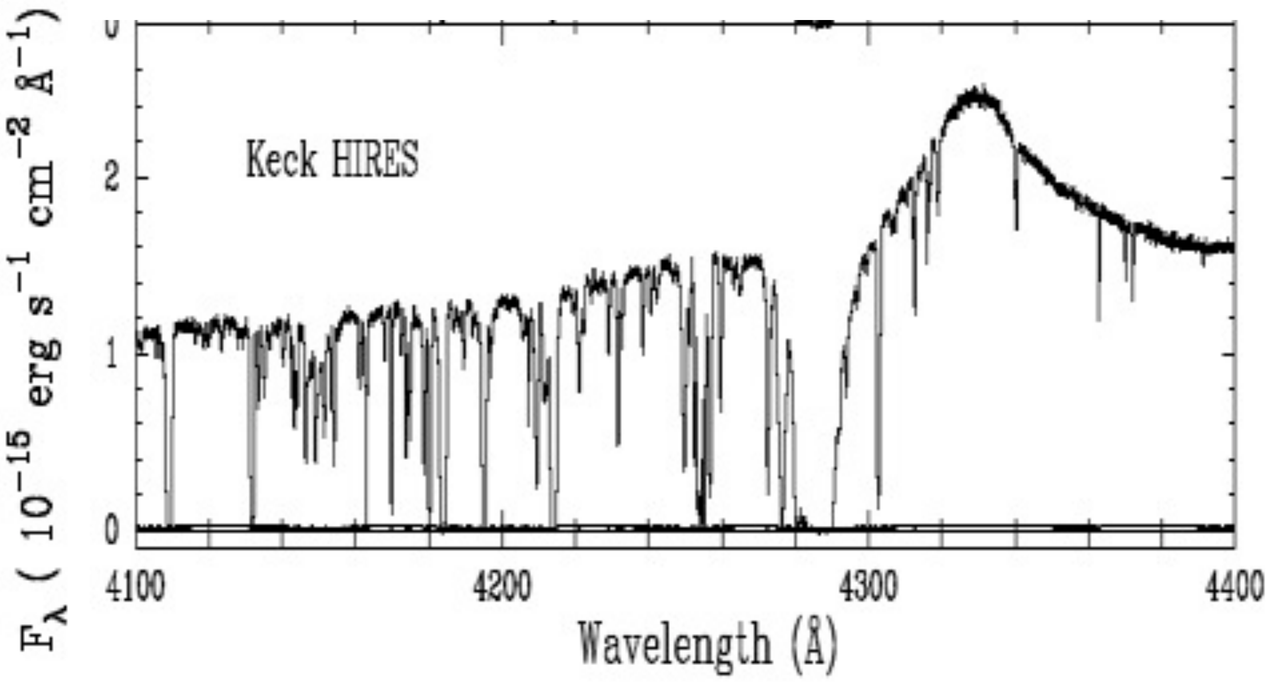

The Lyα absorption near 4285 Å is from the system in which we measure D/H.

The detection of Deuterium and the modeling of this system seem convincing. This is just a portion of the evidence that the Tytler group presented in this paper. They have similarly convincing evidence for several other Lyman alpha clouds in quasar spectra.

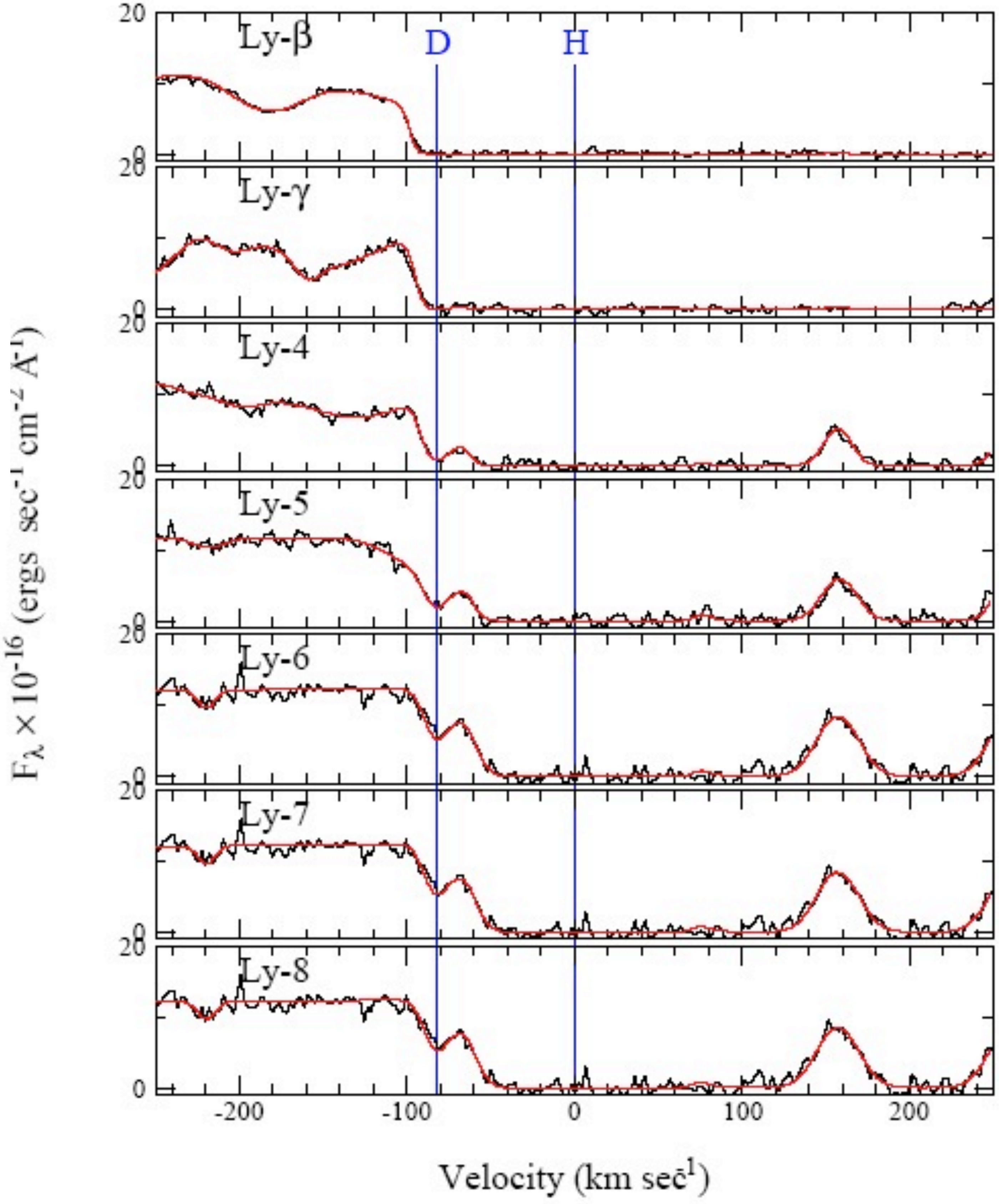

FIG. 7.— The HIRES spectrum of Ly-2 to 8, together with our model of the system, as given in Table 3.

Kirkman, Tytler, Suzuki, O'Meara, & Lubin 2004

The Astrophysical Journal, 781:31 (16pp), 2014 January 20

PRECISION MEASURES OF THE PRIMORDIAL ABUNDANCE OF DEUTERIUM

Ryan J. Cooke, Max Pettini, Regina A. Jorgenson, Michael T. Murphy, and Charles C. Steidel

ABSTRACT

We report the discovery of deuterium absorption in the very metal-poor ([Fe/H] = −2.88) damped Lyα system at zabs = 3.06726 toward the QSO SDSS J1358+6522. On the basis of 13 resolved D i absorption lines and the damping wings of the H i Lyα transition, we have obtained a new, precise measure of the primordial abundance of deuterium. Furthermore, to bolster the present statistics of precision D/H measures, we have reanalyzed all of the known deuterium absorption-line systems that satisfy a set of strict criteria. We have adopted a blind analysis strategy (to remove human bias) and developed a software package that is specifically designed for precision D/H abundance measurements. For this reanalyzed sample of systems, we obtain a weighted mean of (D/H)p = $(2.53 \pm 0.04) \times 10^{-5}$, corresponding to a universal baryon density $100\ \Omega_{b,0}\ h^2 = 2.202 \pm 0.046$ for the standard model of big bang nucleosynthesis (BBN). By combining our measure of (D/H)p with observations of the cosmic microwave background (CMB), we derive the effective number of light fermion species, $N_{\rm eff} = 3.28 \pm 0.28$. We therefore rule out the existence of an additional (sterile) neutrino (i.e., $N_{\rm eff} = 4.046$) at 99.3% confidence...

Montage of the full Lyman series absorption in the DLA at zabs = 3.067259 toward J1358+6522. The black histogram shows the data, fully adjusted to the best-fitting continuum and zero levels, while the red continuous line is the model fit. The minimum χ^2/dof for this fit is 6282.3/6401. Tick marks above the spectrum indicate the location of the velocity components (red ticks for H I, green ticks for D I).

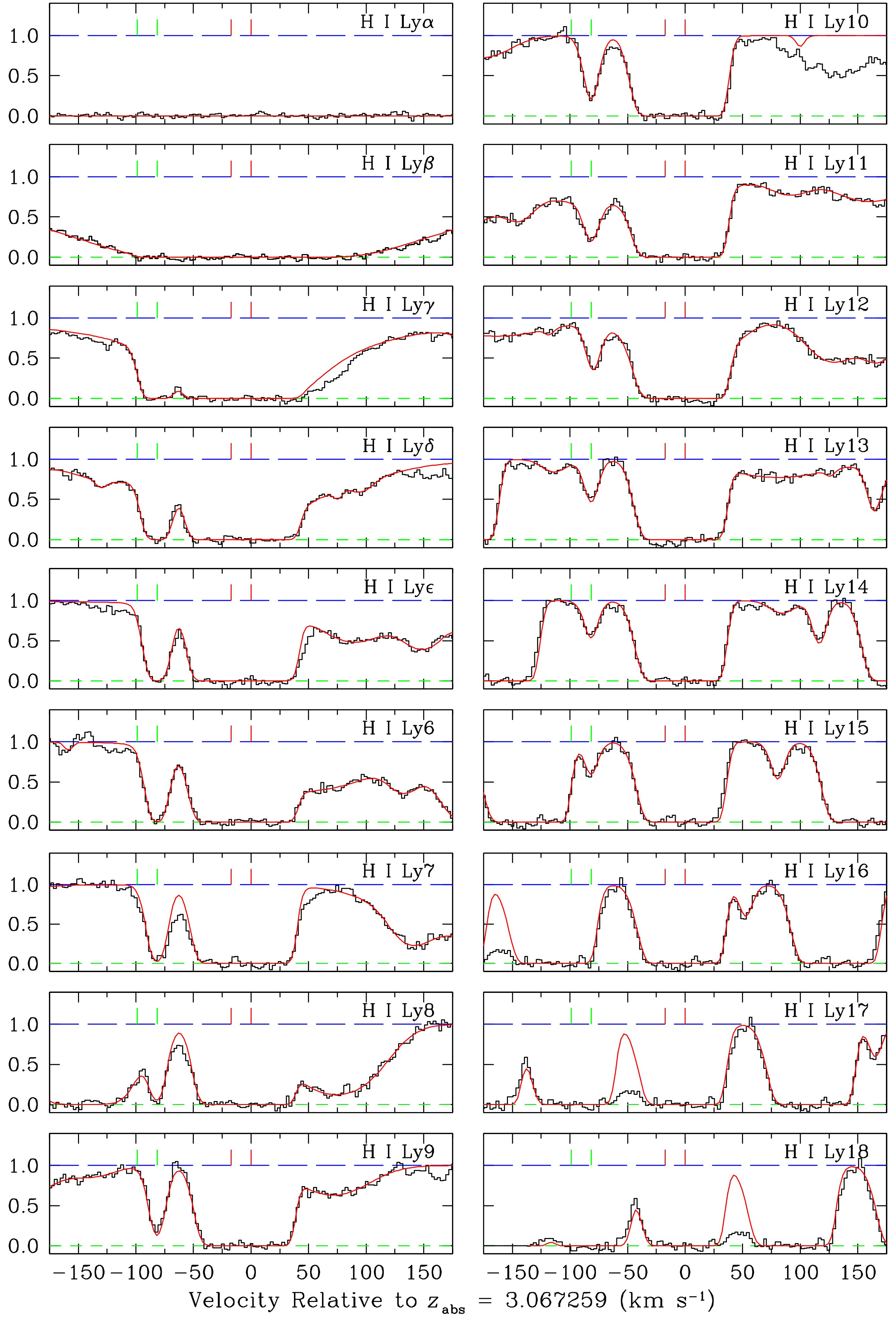

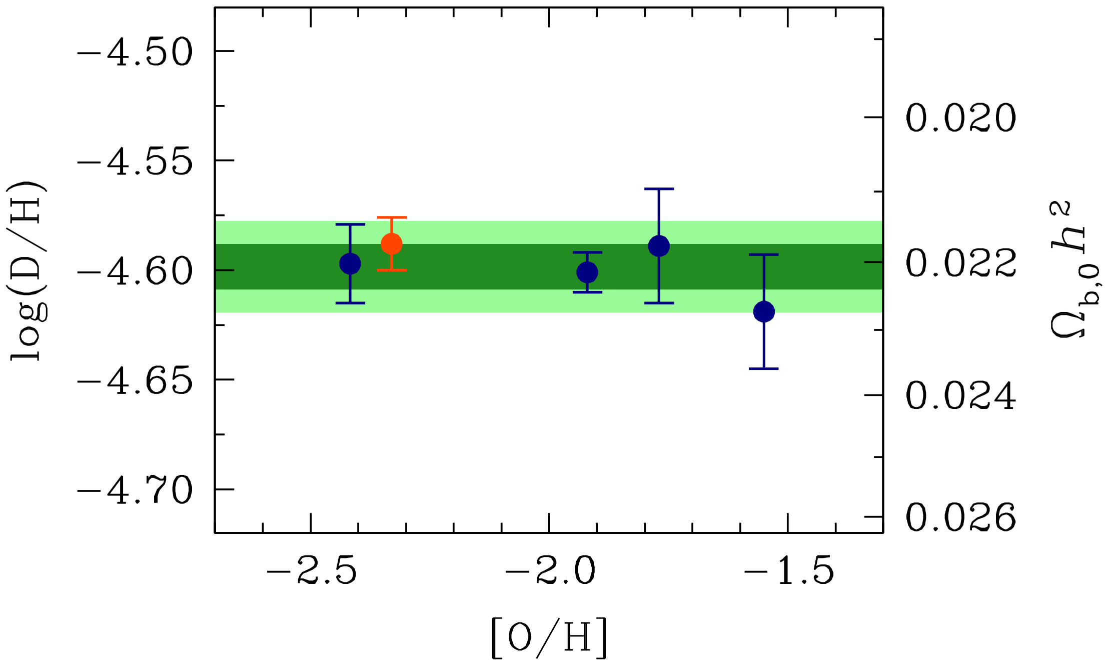

Values of D/H for the Precision Sample of DLA measurements analyzed in this paper. The orange point represents the new case reported here (J1358+6522).

The Li abundance disagreement with BBN may be caused by stellar diffusion

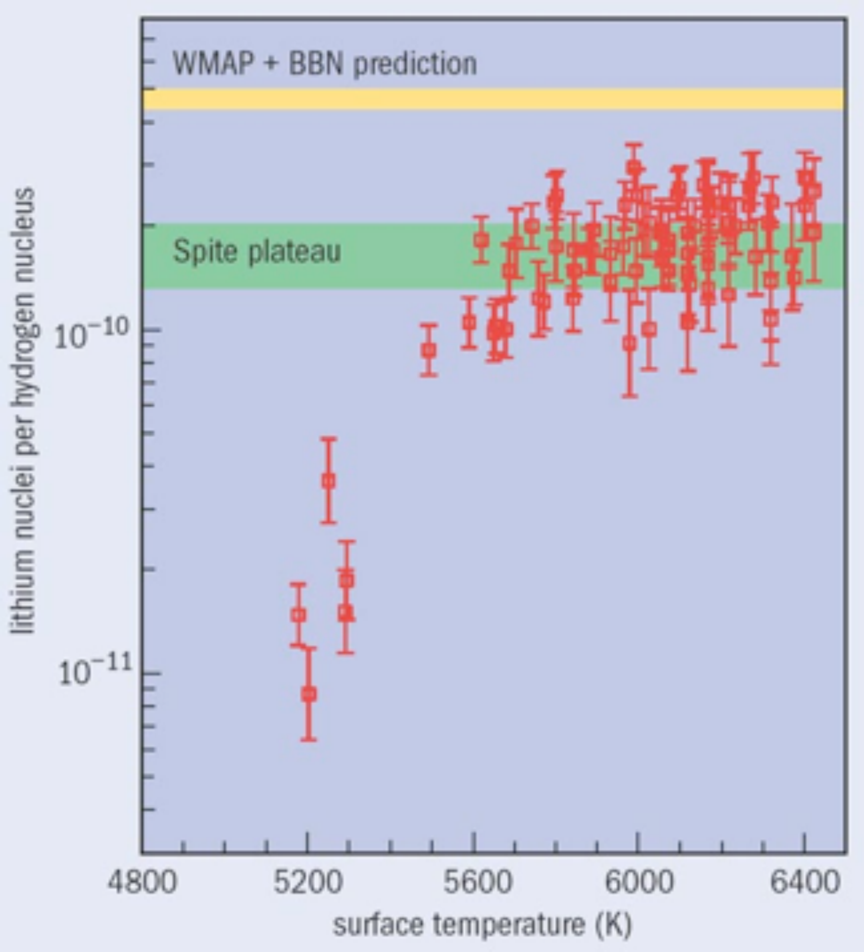

Lithium abundance in very old stars that formed from nearly primordial gas. The amount of ^{7}Li in these "Spite-plateau" stars (green) is much less than has been inferred by combining BBN with measurements of the cosmic microwave background made using WMAP (yellow band). Our understanding of stellar astrophysics may be at fault. Those Spite-plateau stars that have surface temperatures between 5700 and 6400 K have uniform abundances of ^{7}Li because the shallow convective envelopes of these warm stars do not penetrate to depths where the temperature exceeds that for ^{7}Li to be destroyed ($T_{destruct} = 2.5 \times 10^6$ K). The envelopes of cooler stars (data points towards the left of the graph) do extend to such depths, so their surfaces have lost ^{7}Li to nuclear reactions. **If the warm stars gradually circulate ^{7}Li from the convective envelope to depths where $T > T_{destruct}$, then their surfaces may also slowly lose their ^{7}Li.** From http://physicsworld.com/cws/article/print/30680

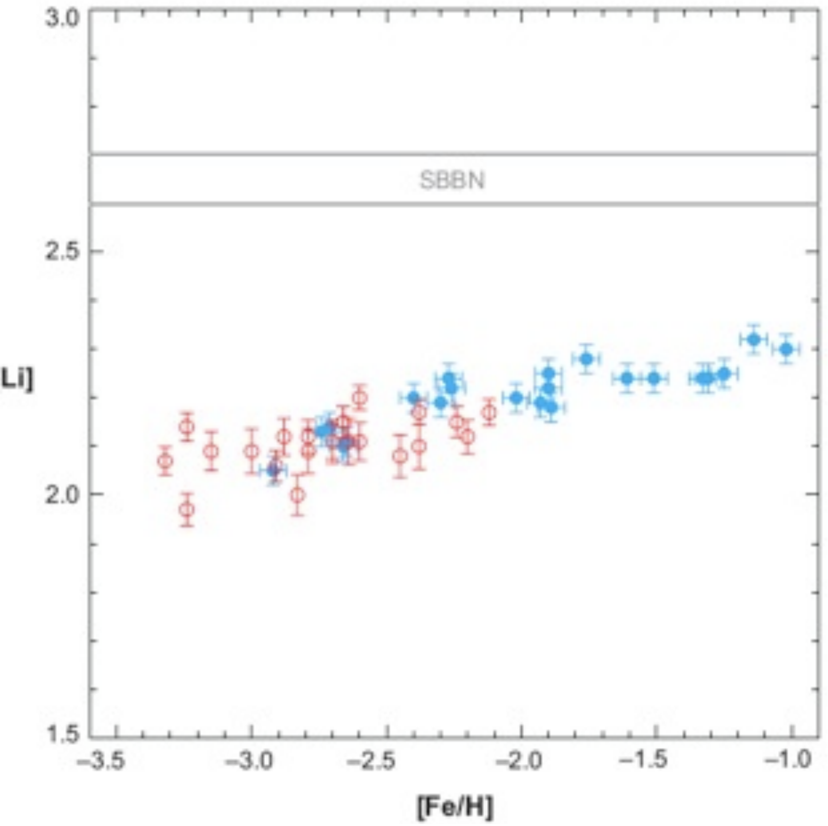

Lithium abundances, [Li] ≡ 12+ log(Li/H), versus metallicity (on a log scale relative to solar) from (red) S. Ryan et al. 2000, ApJ, 530, L57; (blue) M. Asplund et al.2006, ApJ, 644, 229. Figure from G. Steigman 2007, ARAA 57, 463. **Korn et al. 2006 find that both lithium and iron have settled out of the atmospheres of these old stars, and they infer for the unevolved abundances, [Fe/H] = –2.1 and [Li] = 2.54 ± 0.10, in excellent agreement with SBBN.**

The most stringent constraint on a mixing model is that it must maintain the observed tight bunching of plateau stars that have the same average ^{7}Li abundance. In a series of papers that was published between 2002 and 2004, Olivier Richard and collaborators at the Université de Montréal in Canada proposed such a mixing model that has since gained observational support. It suggests that all nuclei heavier than hydrogen settle very slowly out of the convective envelope under the action of gravity. In particular, the model makes specific predictions for settling as a star evolves, which are revealed as variations of surface composition as a function of mass in stars that formed at the same time.

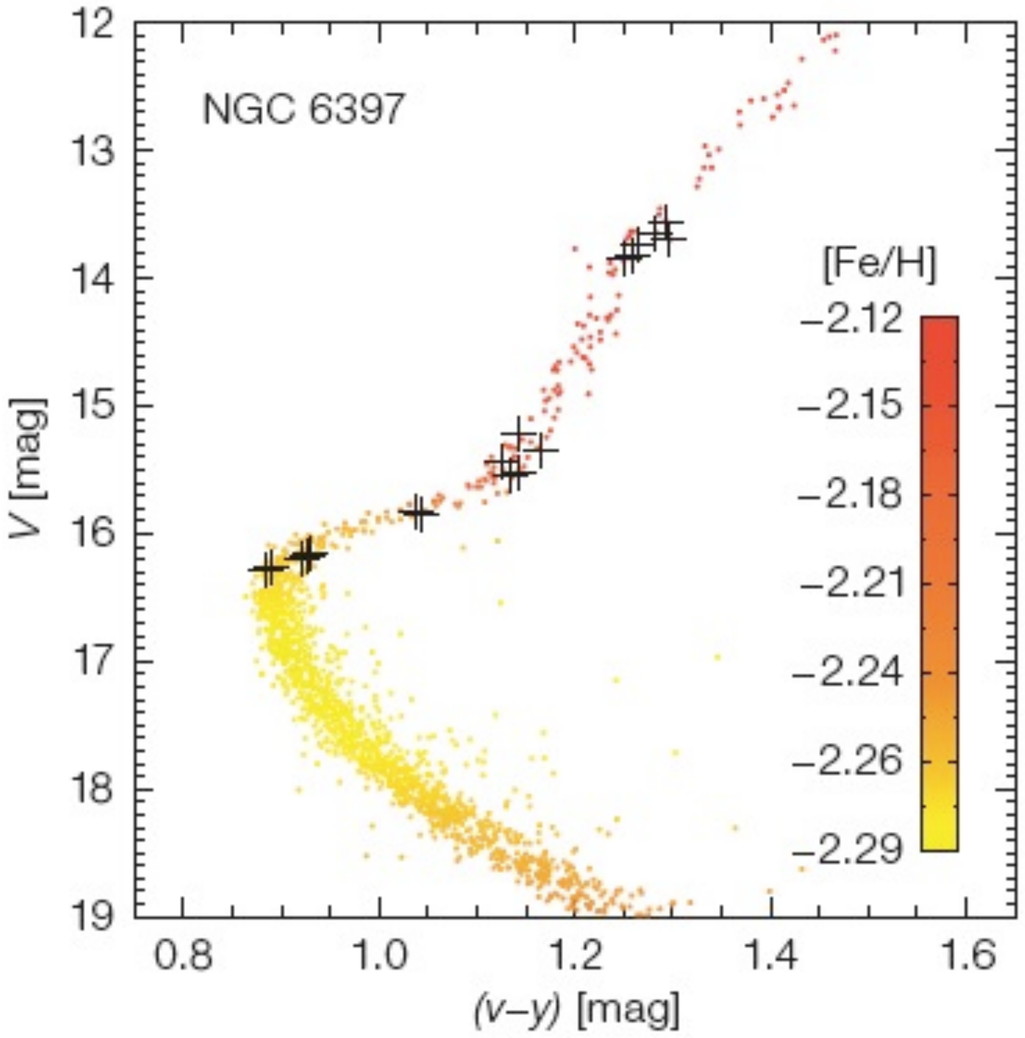

Korn et al. The Messenger 125 (Sept 2006);
Korn et al. 2006, Nature 442, 657.

By spring 2006, Andreas Korn of Uppsala University in Sweden and colleagues had used the European Southern Observatory's Very Large Telescope (VLT) in Chile to study 18 chemically primitive stars in a distant globular cluster called NGC 6397 that were known to have the same age and initial composition. From this Korn et al. showed that the iron and lithium abundances in these stars both varied according to stellar mass as predicted by Richard's model. In fact, the model indicated that the observed stars started out with a ^{7}Li abundance that agrees with the WMAP data. Corroboration of these results is vital because **if the result stands up to scrutiny based on a wide range of data, then we have solved the lithium problem.**

Nature **442**, 657-659 (10 August 2006)

A probable stellar solution to the cosmological lithium discrepancy

A Korn et al.

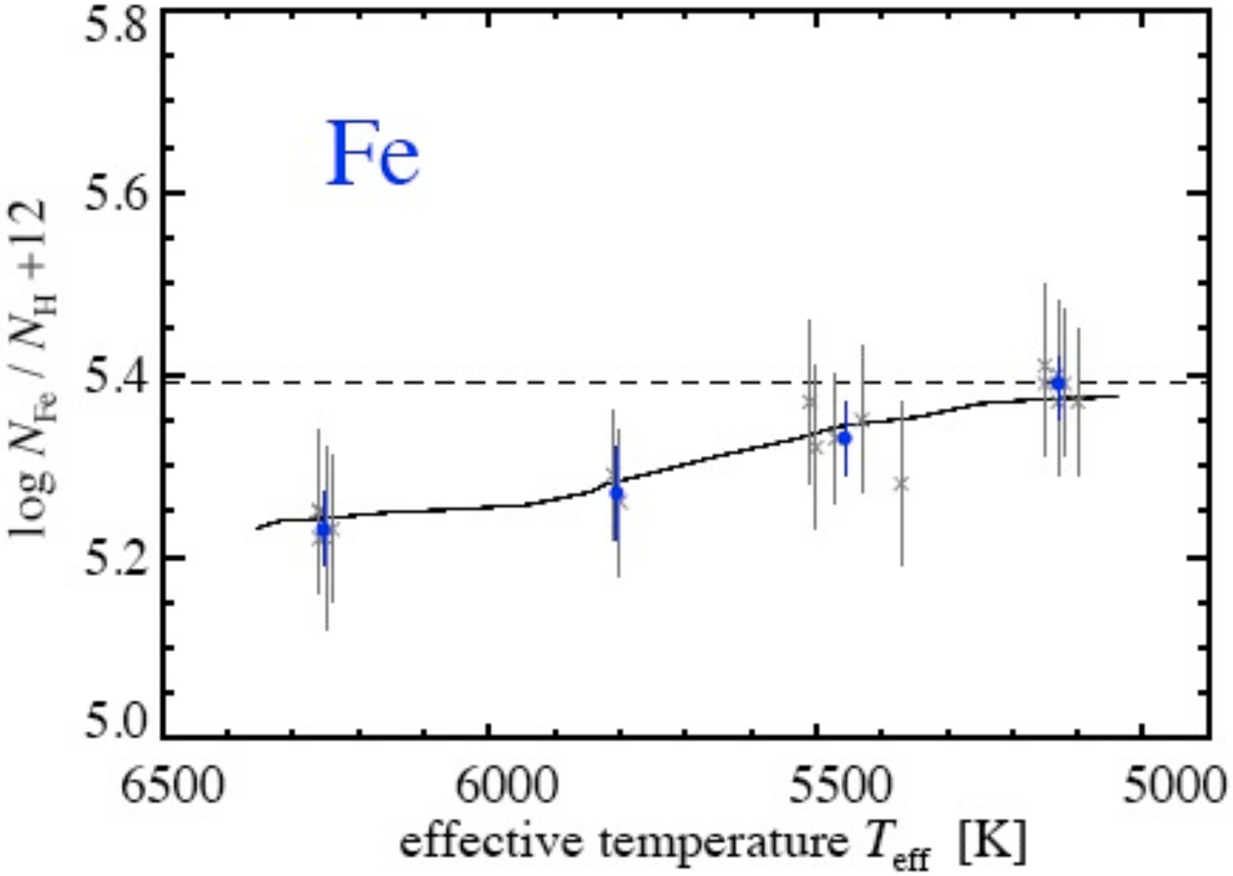

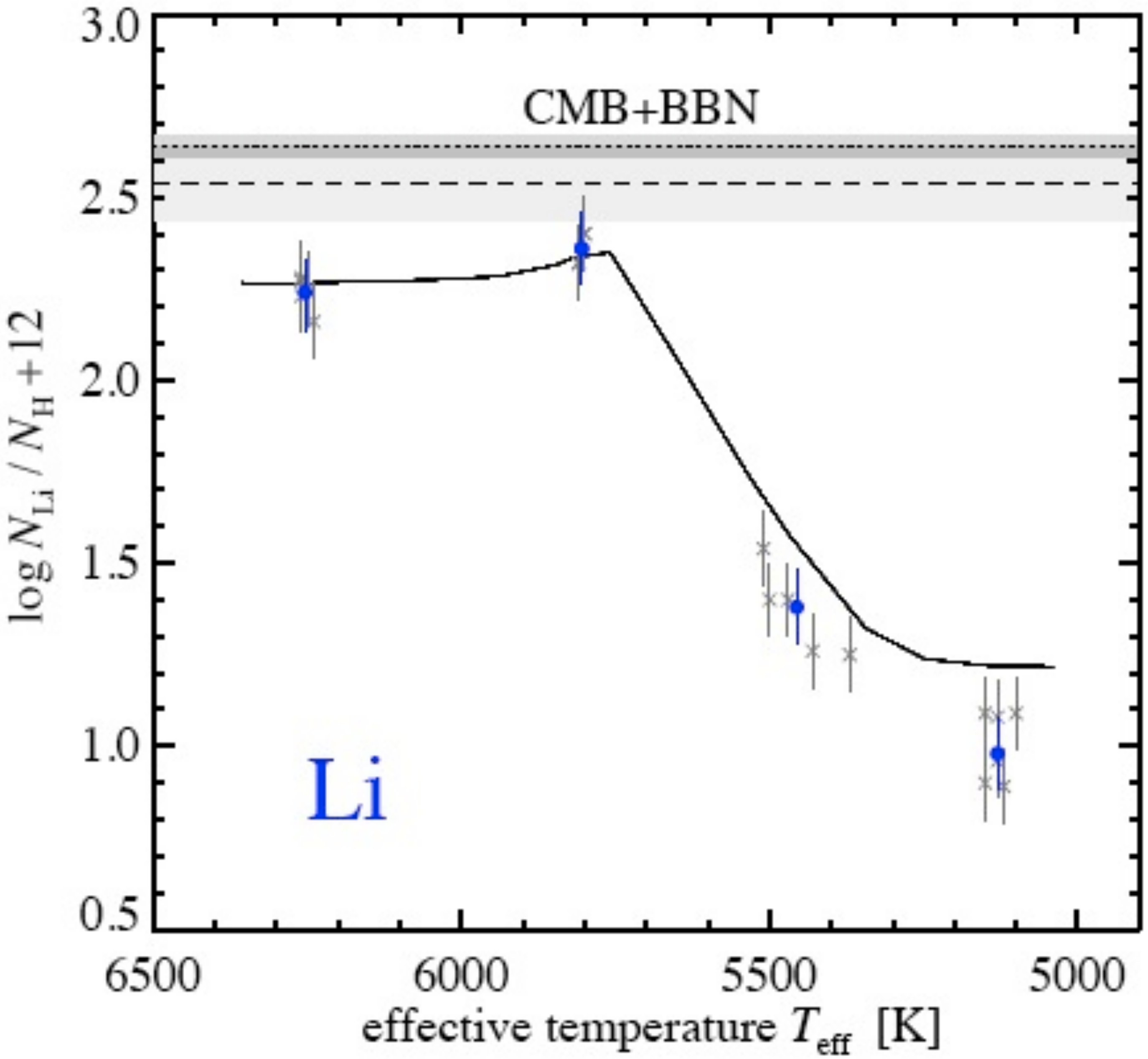

Figure 1: Trends of iron and lithium as a function of the effective temperatures of the observed stars compared to the model predictions. The grey crosses are the individual measurements, while the bullets are the group averages. The solid lines are the predictions of the diffusion model, with the original abundance given by the dashed line. In *b*, the grey-shaded area around the dotted line indicates the 1σ confidence interval of CMB + BBN[1]: $\log[\varepsilon(\mathrm{Li})] = \log(N_{\mathrm{Li}}/N_{\mathrm{H}}) + 12 = 2.64 \pm 0.03$. In *a*, iron is treated in non-equilibrium[20] (non-LTE), while in *b*, the equilibrium (LTE) lithium abundances are plotted, because the combined effect of 3D and non-LTE corrections was found to be very small[29]. For iron, the error bars are the line-to-line scatter of Fe I and Fe II (propagated into the mean for the group averages), whereas for the absolute lithium abundances 0.10 is adopted. The 1σ confidence interval around the inferred primordial lithium abundance ($\log[\varepsilon(\mathrm{Li})] = 2.54 \pm 0.10$) is indicated by the light-grey area.We attribute the modelling shortcomings with respect to lithium in the bRGB and RGB stars to the known need for extra mixing[30], which is not considered in the diffusion model.

Recent references on BBN and Lithium

M Asplund et al. 2006, “Lithium isotopic abundances in metalpoor halo stars” ApJ 644 229–259

A Korn et al. 2006 “A probable stellar solution to the cosmological lithium discrepancy” Nature 442, 657–659; 2007 “Atomic Diffusion and Mixing in Old Stars. I. Very Large Telescope FLAMES-UVES Observations of Stars in NGC 6397” ApJ 671, 402

C Charbonnel 2006, “Where all the lithium went” Nature 442, 636-637

K Nollett 2007, “Testing the elements of the Big Bang” physicsworld.com

R H Cyburt, B D Fields, K A Olive 2008, “An update on the big bang nucleosynthesis prediction for 7Li: the problem worsens” JCAP 11, 12 (also arXiv:0808.2818)

A J Korn 2008 “Atomic Diffusion in Old Stars --- Helium, Lithium and Heavy Elements” ASPC 384, 33

J Melendez et al. 2010 “Observational Signatures for Depletion in the Spite Plateau: Solving the Cosmological Li Discrepancy?” IAU Symposium 268, 211

M Prospelov and J Pradler 2010 “Big Bang Nucleosynthesis as a Probe of New Physics” Annual Reviews of Nuclear and Particle Physics (also on astro-ph)

B Fields 2011 “The Primordial Li Problem” Annual Reviews of Nuclear and Particle Science (also on astro-ph)

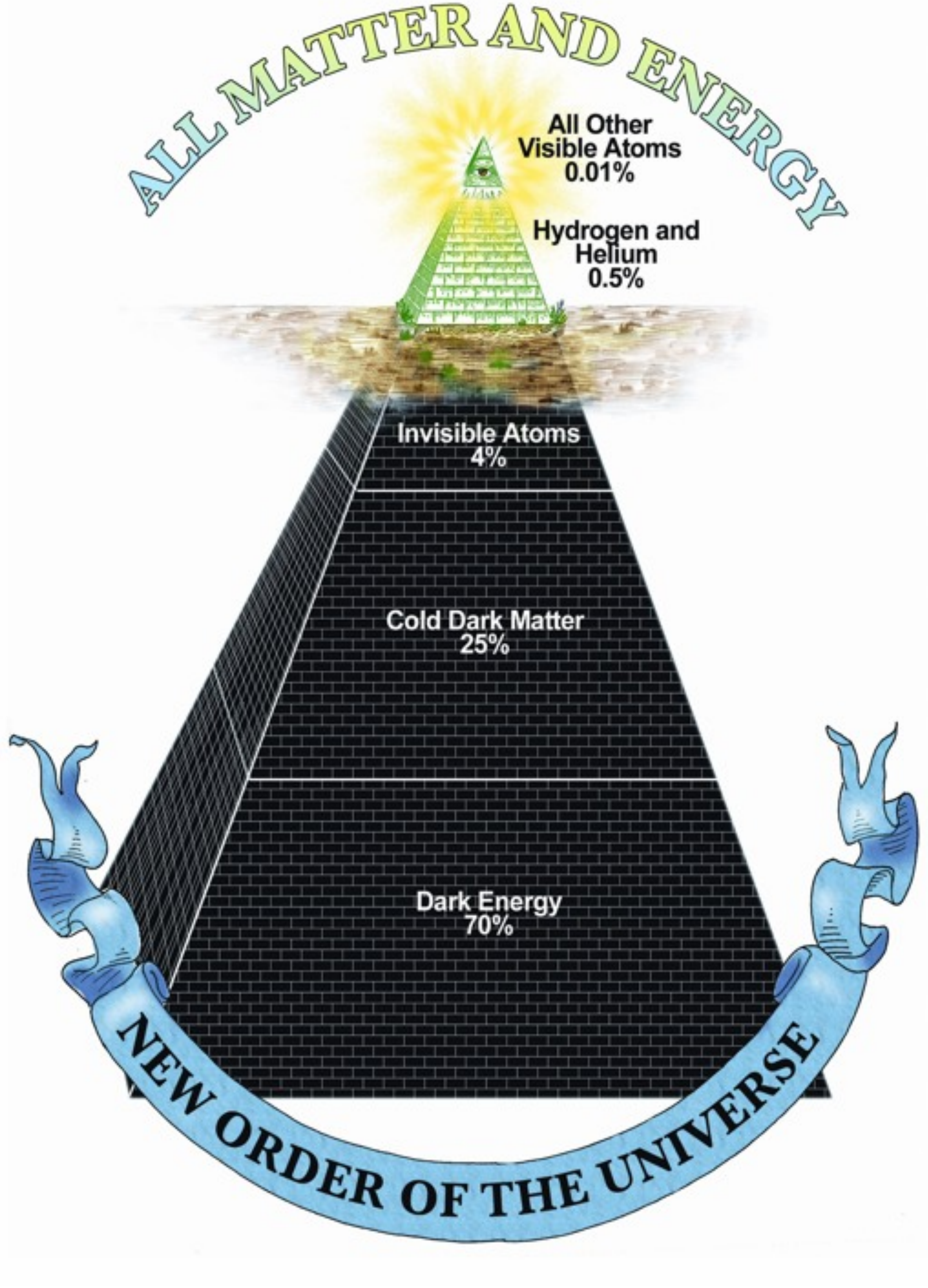

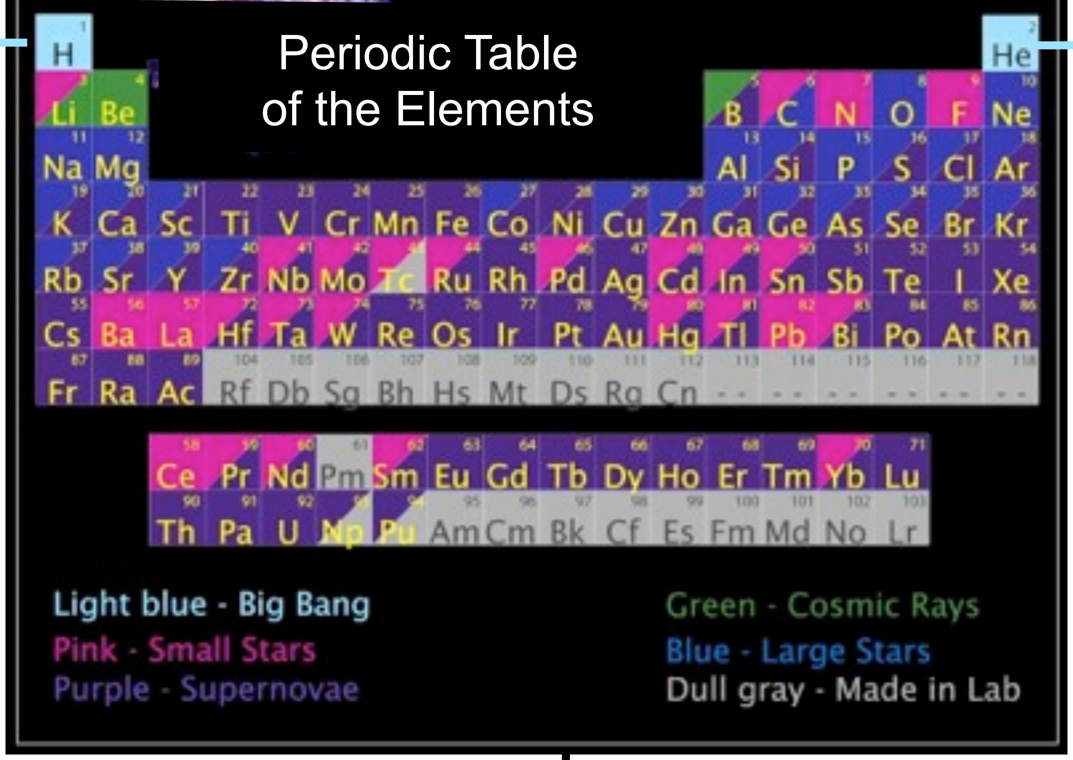

Periodic Table of the Elements

H																	He
Li	Be											B	C	N	O	F	Ne
Na	Mg											Al	Si	P	S	Cl	Ar
K	Ca	Sc	Ti	V	Cr	Mn	Fe	Co	Ni	Cu	Zn	Ga	Ge	As	Se	Br	Kr
Rb	Sr	Y	Zr	Nb	Mo	Tc	Ru	Rh	Pd	Ag	Cd	In	Sn	Sb	Te	I	Xe
Cs	Ba	La	Hf	Ta	W	Re	Os	Ir	Pt	Au	Hg	Tl	Pb	Bi	Po	At	Rn
Fr	Ra	Ac	Rf	Db	Sg	Bh	Hs	Mt	Ds	Rg	Cn	- -	- -	- -	- -	- -	- -
		Ce	Pr	Nd	Pm	Sm	Eu	Gd	Tb	Dy	Ho	Er	Tm	Yb	Lu		
		Th	Pa	U	Np	Pu	Am	Cm	Bk	Cf	Es	Fm	Md	No	Lr		

Light blue - Big Bang

Pink - Small Stars

Purple - Supernovae

Green - Cosmic Rays

Blue - Large Stars

Dull gray - Made in Lab

The Archaeology of the Stars NYTimes 11 Feb 2014 (excerpt)

Anna Frebel, of M.I.T., uses powerful telescopes and high-resolution spectroscopes to study stars' chemical composition.

Four years ago, Anna Frebel, a young astronomer at MIT, found an ancient star in a neighboring galaxy whose chemical composition proved nearly identical to some unusual stars on the outskirts of our own galaxy, which are older than the Milky Way itself.

It was a striking discovery suggesting that the relatively young Milky Way is growing by conquest — "cannibalizing" nearby older dwarf galaxies. And it underscored the importance of a new way of learning how the universe evolved from the Big Bang to the modern cosmos.

Traditionally, astronomers study the early universe by looking back in time — peering deeper and deeper into space for vestiges of light from billions of years ago. But in the last decade, Dr. Frebel and others have used powerful telescopes and high-resolution spectroscopes to study the chemical composition of very old stars closer to home, in the Milky Way's halo, producing a wealth of information about the creation of elements and the formation of the first stars and galaxies.

These astronomers are like Egyptologists combing the desert for relics of bygone civilizations, and call themselves stellar archaeologists. Their work relies on the fact that the rare, primordial stars they are looking for have very few atoms heavier than hydrogen and helium, the gases from which they came together. By contrast, our sun and other relatively young stars are rich in other elements, which astronomers collectively refer to as metals.
Astronomers believe that some of the old stars formed from the chemically enriched dust left over from the explosive deaths of the very first generation of stars, and their atmospheres contain important information about their forebears, like DNA passed from parent to offspring.

A survey of the southern sky in the 1990s produced a trove of potential metal-poor stars. In 2002, Norbert Christlieb at the University of Hamburg in Germany announced that one of them, 36,000 light-years away in the constellation Phoenix, in the Milky Way's galactic halo, had a metallicity of –5.2 — a "relic from the dawn of time," as the journal Nature put it.

Until last week, that star was the most iron-poor astronomers had found. Then, on Sunday, astronomers announced a record. In a paper in Nature, Dr. Frebel and a group of colleagues, including Stefan Keller of Australian National University, the lead author, described a star in the Milky Way constellation Hydrus with a metallicity of less than –7.1 (only an upper limit could be determined).

http://physics.ucsc.edu/~joel/Phys129/StellarArchaeology-NYTimes-11Feb2014.pdf